

# 1 Weak precipitation, warm winters and springs impact 2 glaciers of south slopes of Mt. Everest (central Hima- 3 laya) in the last two decades (1994-2013)

4 Franco Salerno<sup>(1,4\*)</sup>, Nicolas Guyennon<sup>(2)</sup>, Sudeep Thakuri<sup>(1,4)</sup>, Gaetano Viviano<sup>(1)</sup>,  
5 Emanuele Romano<sup>(2)</sup>, Elisa Vuillermoz<sup>(4)</sup>, Paolo Cristofanelli<sup>(3,4)</sup>, Paolo Stocchi<sup>(3)</sup>,  
6 Giacomo Agrillo<sup>(3)</sup>, Yaoming Ma<sup>(5)</sup>, Gianni Tartari<sup>(1,4)</sup>

7 <sup>(1)</sup> National Research Council, Water Research Institute, Brugherio (IRSA -CNR), Italy

8 <sup>(2)</sup> National Research Council, Water Research Institute, Roma (IRSA-CNR), Italy

9 <sup>(3)</sup> National Research Council, Institute of Atmospheric Sciences and Climate (ISAC-CNR) Bologna,  
10 Italy

11 <sup>(4)</sup> Ev-K2-CNR Committee, Via San Bernardino, 145, Bergamo 24126, Italy

12 <sup>(5)</sup> Institute of Tibetan Plateau Research, Chinese Academy of Science, China

13 \*Correspondence to Franco Salerno

14 Email: salerno@irsa.cnr.it

15 Address: IRSA-CNR Via Del Mulino 19. Località Occhiate 20861Brugherio (MB)

16 Phone: +39 039 21694221

17 Fax: +39 039 2004692

## 18 Abstract

19 Studies on recent climate trends from the Himalayan range are limited, and even  
20 completely absent at high elevation (> 5000 m a.s.l.). This study specifically explores  
21 the southern slopes of Mt. Everest, analyzing the time series of temperature and  
22 precipitation reconstructed from seven stations located between 2660 and 5600 m a.s.l.  
23 during 1994-2013, complemented with the data from all existing ground weather  
24 stations located on both sides of the mountain range (Koshi Basin) over the same  
25 period. Overall we find that the main and most significant increase in temperature is  
26 concentrated outside of the monsoon period. Above 5000 m a.s.l. the increasing trend in  
27 the time series of minimum temperature (+0.072 °C y<sup>-1</sup>) is much stronger than of  
28 maximum temperature (+0.009 °C y<sup>-1</sup>), while the mean temperature increased by +0.044  
29 °C y<sup>-1</sup>. Moreover, we note a substantial liquid precipitation weakening (-9.3 mm y<sup>-1</sup>)  
30 during the monsoon season. The annual rate of decrease in precipitation at higher  
31 elevations is similar to the one at lower elevations on the southern side of the Koshi  
32 Basin, but the drier conditions of this remote environment make the fractional loss  
33 much more consistent (-47% during the monsoon period). Our results challenge the  
34 assumptions on whether temperature or precipitation is the main driver of recent glacier  
35 mass changes in the region. The main implications are the following: (1) the negative  
36 mass balances of glaciers observed in this region can be more ascribed to a decrease in  
37 accumulation (snowfall) than to an increase in surface melting; (2) the melting has only

38 been favored during winter and spring months and close to the glaciers terminus; (3) a  
39 decrease in the probability of snowfall (-10%) has made a significant impact only at  
40 glacier ablation zone, but the magnitude of this decrease is distinctly lower than the  
41 observed decrease in precipitation; (4) the decrease in accumulation could have caused  
42 the observed decrease in glacier flow velocity and the current stagnation of glacier  
43 termini, which in turn could have produced more melting under the debris glacier cover,  
44 leading to the formation of numerous supraglacial and proglacial lakes that have  
45 characterized the region in the last decades.

46  
47 ~~Studies on recent climate trends from the Himalayan range are limited, and even~~  
48 ~~completely absent at high elevation. This contribution specifically explores the southern~~  
49 ~~slopes of Mt. Everest (central Himalaya), analyzing the minimum, maximum, and mean~~  
50 ~~temperature and precipitation time series reconstructed from seven stations located~~  
51 ~~between 2660 and 5600 m a.s.l. over the last twenty years (1994-2013). We complete~~  
52 ~~this analysis with data from all the existing ground weather stations located on both~~  
53 ~~sides of the mountain range (Koshi Basin) over the same period. Overall we observe~~  
54 ~~that the main and more significant increase in temperature is concentrated outside of the~~  
55 ~~monsoon period. At higher elevations minimum temperature ( $0.072 \pm 0.011 \text{ }^\circ\text{C a}^{-1}$ ,  $p <$   
56  $0.001$ ) increased far more than maximum temperature ( $0.009 \pm 0.012 \text{ }^\circ\text{C a}^{-1}$ ,  $p >$   
57  $0.1$ ), while mean temperature increased by  $0.044 \pm 0.008 \text{ }^\circ\text{C a}^{-1}$ ,  $p <$   
58  $0.05$ . Moreover, we note a substantial precipitation weakening ( $9.3 \pm 1.8 \text{ mm a}^{-1}$ ,  $p <$   
59  $0.01$  during the monsoon season). The annual rate of decrease at higher elevation is similar to the one at lower  
60 altitudes on the southern side of the Koshi Basin, but here the drier conditions of this  
61 remote environment make the fractional loss much more consistent (47% during the  
62 monsoon period). This study contributes to change the perspective on which climatic  
63 driver (temperature vs. precipitation) led mainly the glacier responses in the last twenty  
64 years. The main implications are the following: 1) the negative mass balances of  
65 glaciers observed in this region can be more ascribed to less accumulation due to  
66 weaker precipitation than to an increase of melting processes. 2) The melting processes  
67 have only been favored during winter and spring months and close to the glaciers  
68 terminus. 3) A decreasing of the probability of snowfall has significantly interested only  
69 the glaciers ablation zones (10 %,  $p <$  0.05), but the magnitude of this phenomenon is  
70 decidedly lower than the observed decrease of precipitation. 4) The lesser accumulation  
71 could be the cause behind the observed lower glacier flow velocity and the current  
72 stagnation condition of tongues, which in turn could have triggered melting processes  
73 under the debris glacier coverage, leading to the formation of numerous supraglacial  
74 and proglacial lakes that have characterized the region in the last decades. Without  
75 demonstrating the causes that could have led to the climate change pattern observed at  
76 high elevation, we conclude by listing the recent literature on hypotheses that accord  
77 with our observations.~~

78 **Keywords:** temperature lapse rate, precipitation gradient, monsoon weakening,  
79 Sequential Mann-Kendall, expectation maximization algorithm, climate change, glaciers  
80 shrinkage, central Himalaya

## 81 **1 Introduction**

82 The current uncertainties concerning the glacial shrinkage in the Himalayas are  
83 mainly attributed to a lack of measurements, both of the glaciers and of climatic forcing  
84 agents (e.g., Bolch et al., 2012). Recent results underline the need for a fine scale inves-  
85 tigation, especially at high altitude, to better model the hydrological dynamics in this ar-  
86 ea. However, there are few high elevation weather stations in the world where the glaci-  
87 ers are located (Tartari et al., 2009). This can be attributed to the remote location of  
88 glaciers, the rugged terrain, and a complex political situation, all of which make phys-  
89 ical access difficult (Bolch et al., 2012). As a consequence of the remoteness and diffi-  
90 culty in accessing many high elevation sites combined with the complications of operat-  
91 ing automated weather stations (AWSs) at these altitudes, long-term measurements are  
92 challenging (Vuille, 2011). However, nearly all global climate models report increased  
93 sensitivity to warming at high elevations (e.g., Rangwala and Miller, 2012), while ob-  
94 servations are less clear (Pepin and Lundquist, 2008). Moreover, changes in the timing or  
95 amount of precipitation are much more ambiguous and difficult to detect, and there is  
96 no clear evidence of significant changes in total precipitation patterns in most mountain  
97 regions (Vuille, 2011).

98 The need for a fine scale investigation is particularly evident on the south slope of  
99 Mt. Everest (central Southern Himalaya, CH-S) as it is one of the heavily glaciated parts  
100 of the Himalaya (Salerno et al., 2012; Thakuri et al., 2014). Nevertheless, these glaciers  
101 have the potential to build up moraine-dammed lakes storing large quantities of water,  
102 which are susceptible to GLOFs (glacial lake outburst floods) (e.g., Salerno et al., 2012;  
103 Fujita et al., 2013). Gardelle et al. (2011) noted that this region is most characterized by  
104 glacial lakes in the Hindu Kush Karakorum Himalaya. Recently, Thakuri et al. (2014)  
105 noted that the Mt. Everest glaciers experienced an accelerated shrinkage in the last  
106 twenty years (1992-2011), as underlined by an upward shift of the Snow Line Altitude  
107 (SLA) with a velocity almost three times greater than the previous period (1962-1992).  
108 Furthermore Bolch et al. (2011) and Nuimura et al. (2012) found a higher mass loss rate  
109 during the last decade (2000–2010). Anyway, to date, there are not continuous  
110 meteorological time series able to clarify the causes of the melting process to which the  
111 glaciers of these slopes are subjected.

112 In this context, since the early 1990s, PYRAMID Observatory Laboratory (5050 m  
113 [a.s.l.](http://www.evk2cnr.org)) was created by the *Ev-K2-CNR Committee* ([www.evk2cnr.org](http://www.evk2cnr.org)). This observatory  
114 is located at the highest elevation at which weather data has ever been collected in the  
115 region and thus represents a valuable dataset with which to investigate the climate  
116 change in CH-S (Tartari et al., 2002; Lami et al., 2010). However, the remoteness and  
117 the harsh conditions of the region over the years have complicated the operations of the  
118 AWSs, obstructing long-term measurements from a unique station.

119 In this paper, we mainly explore the small scale climate variability of the south  
120 slopes of Mt. Everest by analyzing the minimum, maximum, and mean air temperature  
121 (T) and liquid precipitation (Prec) time series reconstructed from seven AWSs located  
122 from 2660 to 5600 m a.s.l. over the last couple of decades (1994-2013). Moreover, we  
123 complete this analysis with all existing weather stations located on both sides of the  
124 Himalayan range (Koshi Basin) for the same period. In general, this study has the  
125 ultimate goal of linking the climate change patterns observed at high elevation with the  
126 glacier responses over the last twenty years, during which a more rapid glacier  
127 shrinkage process occurred in the region of investigation.

## 128 **2 Region of investigation**

129 The current study is focused on the Koshi (KO) Basin which is located in the eastern  
130 part of central Himalaya (CH) (Yao et al., 2012; Thakuri et al., 2014). To explore  
131 possible differences in the surroundings of Mt. Everest, we decided to consider the  
132 north and south parts of CH (with the suffixes -N and -S, respectively) separately (Fig.  
133 1a). The KO River (58,100 km<sup>2</sup> of the basin) originates in the Tibetan Plateau (TP) and  
134 the Nepali highlands. The area considered in this study is within the latitudes of 27° and  
135 28.5° N and longitudes of 85.5° and 88° E. The altitudinal gradient of this basin is the  
136 highest in the world, ranging from 77 to 8848 m a.s.l., i.e., Mt. Everest. We subdivide  
137 the KO Basin into the northern side (KO-N), belonging to the CH-N, and southern side  
138 (KO-S), belonging to the CH-S. The southern slopes of Mt. Everest are part of the  
139 Sagarmatha (Everest) National Park (SNP) (Fig. 1b), where the small scale climate  
140 variability at high elevation is investigated. The SNP is the world's highest protected  
141 area, with over 30000 tourists in 2008 (Salerno et al., 2010a; Salerno et al., 2013). The  
142 park area (1148 km<sup>2</sup>), extending from an elevation of 2845 to 8848 m a.s.l., covers the  
143 upper Dudh Koshi (DK) Basin (Manfredi et al., 2010; Amatya et al., 2010). Land cover  
144 classification shows that almost one-third of the territory is characterized by glaciers  
145 and ice cover (Salerno et al., 2008; Tartari et al., 2008), while less than 10% of the park  
146 area is forested (Bajracharya et al., 2010; Salerno et al., 2010b). The SNP presents a  
147 broad range of bioclimatic conditions with three main bioclimatic zones: the zone of  
148 alpine scrub; the upper alpine zone, which includes the upper limit of vegetation  
149 growth; and the Arctic zone, where no plants can grow (UNEP and WCMC, 2008).  
150 Figure 1c shows the glacier distribution along the hypsometric curve of the SNP. We  
151 observe that the glacier surfaces are distributed from 4300 m to above 8000 m a.s.l.,  
152 with more than 75% of the glacier surfaces lying between 5000 m and 6500 m a.s.l. The  
153 2011 area-weighted mean elevation of the glaciers was 5720 m a.s.l. (Thakuri et al.,  
154 2014). These glaciers are identified as the summer accumulation-type fed mainly by  
155 summer Prec from the South Asian monsoon system, whereas the winter Prec caused by  
156 the mid-latitude westerly wind is minimal (Yao et al., 2012). The prevailing direction of  
157 the monsoons is S-N and SW-NE (e.g., Ichiyanagi et al., 2007). The climate is  
158 influenced by the monsoon system because the area is located in the subtropical zone  
159 with nearly 90% of the annual Prec falling in the months of June to September (this

160 study). Heavy autumn and winter snowfalls can occur in association with tropical  
161 cyclones and westerly disturbances, respectively, and snow accumulation can occur at  
162 high elevations at all times of the year (Benn, 2012). Bollasina et al. (2002) have  
163 demonstrated the presence of well-defined local circulatory systems in the Khumbu  
164 Valley (SNP). The local circulation is dominated by a system of mountain and valley  
165 breezes. The valley breeze blows (approximately  $4 \text{ m s}^{-1}$ ) from the south every day from  
166 sunrise to sunset throughout the monsoon season, pushing the clouds that bring Prec  
167 northward.

### 168 3 Data

#### 169 3.1 Weather stations at high elevation

170 The first automatic weather station (named hereafter AWS0) at 5050 m a.s.l. near  
171 PYRAMID Observatory Laboratory (Fig. 1c), ~~and beginning was established~~ in October  
172 1993, it has run continuously all year round (Bertolani et al., 2000). The station, operat-  
173 ing in extreme conditions, had recorded long-term ground-based ~~meteorological-tem-~~  
174 ~~perature and temperature~~ data, ~~and the data- which~~ are considered valid until December  
175 2005. Due to the obsolescence of technology, the station was disposed of in 2006. A  
176 new station (named hereafter AWS1) was installed just a few tens of meters away from  
177 AWS0 and has been operating since October 2000. Other stations were installed in the  
178 following years in the upper DK Basin in the Khumbu Valley (Table 1). In 2008, the  
179 network included ~~the sixth monitoring points,~~ including the highest weather station of  
180 the world, located at South Col of Mt. Everest (7986 m a.s.l.). The locations of all sta-  
181 tions are presented in Figure 1b. We can observe in Figure 1c that this meteorological  
182 network ~~represents well the climatic conditions~~ ~~represents the climatic conditions~~ of the  
183 SNP glaciers ~~-well~~: AWS0 and AWS1 (5035 m a.s.l.) characterize the glacier fronts  
184 (4870 m a.s.l.), AWS4 (5600 m a.s.l.) represents the mean elevation of glaciers in the  
185 area (5720 m a.s.l.), and AWS5, the surface station at South Col (7986 m a.s.l.), charac-  
186 terizes the highest peaks (8848 m a.s.l.).

187 All stations, except AWS5 (only T), record at least T and Prec. This dataset presents  
188 some gaps (listed in Table 1) as a consequence of the complications of operating AWS  
189 at these altitudes. The list of measured variables for each stations and relevant data can  
190 be downloaded from <http://geonetwork.evk2cnr.org/>. Data processing and quality  
191 checks are performed according to the international standards of the WMO (World Me-  
192 teorological Organization).

193 The Prec sensors at these locations are conventional heated tipping buckets ~~usually~~  
194 ~~used for rainfall measurements and which~~ may not fully capture the solid Prec. There-  
195 fore, solid Prec is probably underestimated, especially in winter. However, in order to  
196 know the magnitude of the possible underestimation of the solid phase, we compared  
197 the monthly mean Prec of the reconstructed PYRAMID series (1994-2013 period) with  
198 the Prec of a station located downstream at 2619 m a.s.l. (Chaurikhark, ID 1202), (Fig.  
199 1b, Table 2) which presents monthly mean temperature above  $0 \text{ }^\circ\text{C}$  even during the win-

200 [ter and thus a high prevalence of liquid Prec also during these months. This comparison,](#)  
201 [supported by the elevated correlation existing between the monthly Prec of the two sta-](#)  
202 [tions, shown a slight underestimation of the PYRAMID snow \(about 3±1% of total an-](#)  
203 [nual precipitation registered at PYRAMID, see Supplementary material 3 for more de-](#)  
204 [tails\). Therefore, being much reduced the underestimation, we decided not to manipu-](#)  
205 [late data. However the trends hereafter reported are referred mainly to the liquid phase](#)  
206 [of Prec.](#) In this regard, according to both Fujita and Sakai, 2014 and field observations  
207 (Ueno et al., 1994), the precipitation phase has been taken into account assuming that  
208 the probability of snowfall and rainfall depends on mean daily [air](#) temperature, using [as](#)  
209 [thresholds](#) – as proposed by the aforementioned authors – ~~as thresholds~~ 0 °C and 4 °C,  
210 respectively. In Figure 2 we first of all observe that at 5050 m a.s.l. 90% of precipitation  
211 is concentrated during June-September and that the probability of snowfall is very low  
212 (4%), considering that the mean daily temperature during these months is above 0 °C.  
213 On a yearly basis, this probability reaches 20% of the annual cumulated precipitation.

### 214 3.2 Other weather stations at lower altitude in the Koshi Basin

215 In KO-S Basin (Nepal), the stations are operated by the Department of Hydrology  
216 and Meteorology (DHM) ([www.dhm.gov.np/](http://www.dhm.gov.np/)). For daily T and Prec, we selected 10  
217 stations for T and 19 stations for Prec considering both the length of the series and the  
218 monitoring continuity (< 10% of missing daily data). The selected stations cover an  
219 elevation range between 158 and 2619 m a.s.l. (Table 3). In KO-N Basin (TP, China),  
220 the number of ground weather stations (operated by the Chinese Academy of Science  
221 (CAS)), selected with the same criteria mentioned above, is considerably smaller, just  
222 two, but these stations have a higher elevation (4302 m [a.s.l.](#) for the Dingri station and  
223 3811 m a.s.l. for the Nyalam station).

224 [The quality insurance of these meteorological data is ensured considering that they](#)  
225 [are used as part of global and regional networks including for instance APHRODITE](#)  
226 [\(Asian Precipitation–Highly Resolved Observational Data Integration Towards](#)  
227 [Evaluation of Water Resources\) \(Yasutomi et al., 2011\) and GHCN \(Global Historical](#)  
228 [Climatology Network\) \(Menne et al., 2012\).](#)

## 229 4 Methods

230 We define the pre-monsoon, monsoon, and post-monsoon seasons as the months  
231 from February to May, June to September, and October to January, respectively. The  
232 minT, maxT, and meanT are calculated as the minimum, maximum, and mean daily air  
233 temperature. For total precipitation (Prec), we calculate the mean of the cumulative  
234 precipitation for the analyzed period.

### 235 4.1 Reconstruction of the daily temperature and precipitation time series at high 236 elevation

237 The two stations named AWS0 and AWS1 in the last twenty years, considering the  
238 extreme weather conditions of ~~these slopes~~this area, present a percentage of missing  
239 daily values of approximately 20% (Table 1). The other stations (hereafter named  
240 secondary stations) were used here for infilling the gaps according to a priority criteria  
241 based on the degree of correlation among data. AWS1 was chosen as the reference  
242 station given the length of the time series and that it is currently still operating.  
243 Therefore, our reconstruction (hereafter named PYRAMID) is referred to an elevation  
244 of 5035 m a.s.l.

245 The selected infilling method is a simple regression analysis based on quantile  
246 mapping (e.g., Déqué, 2007; Themeßl et al., 2012). This ~~simple~~-regression method has  
247 been preferred to more complex techniques, such as the fuzzy rule-based approach  
248 (Abebe et al., 2000) or the artificial neural networks (Abudu et al., 2010; Coulibaly and  
249 Evora, 2007), considering the peculiarity of this case study. In fact, all stations are  
250 located in the same valley (Khumbu Valley). This aspect confines the variance among  
251 the stations to the altitudinal gradient of the considered variable (T or Prec), which can  
252 be easily reproduced by the stochastic link created by the quantile mapping method. In  
253 case all stations registered a simultaneous gap, we apply a multiple imputation  
254 technique (Schneider, 2001) that uses some other proxy variables to fill the remaining  
255 missing data. Details on the reconstruction procedure and the computation of the  
256 associated uncertainty are provided in Supplementary Material 1.

#### 257 4.2 The trends analysis: the Sequential Mann-Kendall test

258 The Mann-Kendall (MK) test (Kendall, 1975) is widely adopted to assess significant  
259 trends in hydro-meteorological time series (e.g., Carraro et al., 2012a, 2012b; Guyennon  
260 et al., 2013). This test is non-parametric, thus being less sensitive to extreme sample  
261 values, and is independent of the hypothesis about the nature of the trend, whether  
262 linear or not. The MK test verifies the assumption of the stationarity of the investigated  
263 series by ensuring that the associated normalized Kendall's tau coefficient,  $\mu(\tau)$ , is  
264 included within the confidence interval for a given significance level (for  $\alpha = 5\%$ , the  
265  $\mu(\tau)$  is below  $-1.96$  and above  $1.96$ ). In the sequential form (seqMK) (Gerstengarde  
266 and Werner, 1999),  $\mu(\tau)$  is calculated for each element of the sample. The procedure  
267 is applied forward starting from the oldest values (progressive) and backward starting  
268 from the most recent values (retrograde). If no trend is present, the patterns of  
269 progressive and retrograde  $\mu(\tau)$  versus time (i.e., years) present several crossing  
270 points, while a unique crossing period allows the approximate location of the starting  
271 point of the trend (e.g., Bocchiola and Diolaiuti, 2010).

272 In this study, the seqMK is applied to monthly vectors. Monitoring the seasonal non-  
273 stationarity, the monthly progressive  $\mu(\tau)$  is reported with a pseudo color code, where  
274 the warm colors represent the positive slopes and cold colors the negative ones. Color  
275 codes associated with values outside of the range  $(-1.96$  to  $1.96)$  possess darker tones to  
276 highlight the trend significance (Salerno et al., 2014). Moreover, to monitor the overall

277 non-stationarity of the time series, both the progressive and the retrograde  $\mu(\tau)$  at the  
278 annual scale are reported. We used the Sen's slope proposed by Sen (1968) as a robust  
279 linear regression allowing the quantification of the potential trends revealed by the  
280 seqMK (e.g., Bocchiola and Diolaiuti, 2010). The significance level is established for  $p$   
281  $< 0.05$ . We define a slight significance for  $p < 0.10$ . The uncertainty associated with the  
282 Sen's slopes (1994-2013) is estimated through a Monte Carlo uncertainty analysis (e.g.,  
283 James and Oldenburg, 1997), described in detail in Supplementary Material 1.

## 284 5 Results

### 285 5.1 Trend analysis at high elevation

286 Figure 3 shows the reconstructed PYRAMID time series for minT, maxT, meanT,  
287 and Prec resulting from the overall infilling process explained in Supplementary  
288 Material 1. Figure 4 analyzes the monthly trends of T and Prec from 1994 to 2013 for  
289 PYRAMID.

#### 290 *Minimum air temperature (minT)*

291 | November ( $+0.17$  °C  $\text{a}^+ \text{y}^{-1}$ ,  $p < 0.01$ ) and December ( $+0.21$  °C  $\text{a}^+ \text{y}^{-1}$ ,  $p < 0.01$ )  
292 present the highest increasing trend, i.e., both these two months experienced about even  
293  $+4$  °C over twenty years (Fig. 4a). In general, the post- and pre-monsoon periods  
294 experience higher and more significant increases than during the monsoon. In particular,  
295 | we note the significant and consistent increase of minT of April ( $+0.10$  °C  $\text{a}^+ \text{y}^{-1}$ ,  $p <$   
296  $0.05$ ). At the annual scale, the bottom graph shows a progressive  $\mu(\tau)$  trend parallel to  
297 the retrograde  $\mu(\tau)$  one for the entire analyzed period, i.e., a continuous tendency of  
298 minT to rise, which becomes significant in 2007, when the progressive  $\mu(\tau)$  assumes  
299 values above  $+1.96$ . On the right, the Sen's slope completes the analysis, illustrating that  
300 | minT is increasing at annual level by  $\pm 0.072 \pm 0.011$  °C  $\text{a}^+ \text{y}^{-1}$ ,  $p < 0.001$ , i.e.,  $+1.44 \pm$   
301  $0.22$  °C over twenty years.

#### 302 *Maximum air temperature (maxT)*

303 The post- and pre-monsoon months show larger increases in maxT, but with lower  
304 magnitudes and significance than we observe for minT (Fig. 4b). The highest increases  
305 | for this variable occurs also for ~~this variable~~ maxT in April, November and December.  
306 | Less expected is the decrease of maxT in May ( $-0.08$  °C  $\text{a}^+ \text{y}^{-1}$ ,  $p < 0.05$ ) and during the  
307 | monsoon months from June to August ( $-0.05$  °C  $\text{a}^+ \text{y}^{-1}$ ,  $p < 0.1$ ). On the annual scale,  
308 the bottom graph shows a continuous crossing of the progressive and retrograde  $\mu(\tau)$   
309 trends until 2007, i.e., a general stationary condition. From 2007 until 2010, the trend  
310 significantly increased, while 2012 and 2013 register a decrease, bringing the  
311 progressive  $\mu(\tau)$  near the stationary condition. In fact, on the right, the Sen's slope  
312 confirms that maxT is at annual level stationary over the twenty years ( $+0.009 \pm 0.012$   
313 | °C  $\text{a}^+ \text{y}^{-1}$ ,  $p > 0.1$ ).

314 *Mean air temperature (meanT)*

315 | Figure 4c, as expected, presents intermediate conditions for meanT ~~than in respect to~~  
316 | ~~for~~ minT and maxT. All months, except May and the monsoon months from June and  
317 | August, register a positive trend (more or less significant). December presents the  
318 | highest a more significant increasing trend ( $\pm 0.17 \text{ }^\circ\text{C a}^+ \text{y}^{-1}$ ,  $p < 0.01$ ), while April  
319 | shows the highest and a more significant increase ( $p < 0.10$ ) during the pre-monsoon  
320 | period. On the annual scale, the bottom graph shows that the progressive  $\mu(\tau)$  trend  
321 | has always increased since 2000 and that it becomes significant beginning in 2008. On  
322 | the right, the Sen's slope concludes this analysis, showing that meanT has been  
323 | significantly increasing by  $\pm 0.044 \pm 0.008 \text{ }^\circ\text{C a}^+ \text{y}^{-1}$ ,  $p < 0.05$ , i.e.,  $+0.88 \pm 0.16 \text{ }^\circ\text{C}$  over  
324 | twenty years.

325 *Total precipitation (Prec)*

326 | In the last years, all cells are blue, i.e., we observe for all months an overall and  
327 | strongly significant decreasing trend of Prec (Fig. 4d). In general, the post- and pre-  
328 | monsoon periods experience more significant decreases, although the monsoon months  
329 | (June-September) register the main Prec losses (e.g. August registers a Prec loss of even  
330 |  $-4.6 \text{ mm a}^+ \text{y}^{-1}$ ). On the annual scale, the bottom graph shows a continuous decreasing  
331 | progressive  $\mu(\tau)$  trend since 2000 that becomes significant beginning in 2005. On the  
332 | right, the Sen's slope notes that the decreasing Prec trend is strongly high and  
333 | significant at annual level ( $-13.7 \pm 2.4 \text{ mm a}^+ \text{y}^{-1}$ ,  $p < 0.001$ ).

334 | The precipitation reduction is mainly due to a reduction in intensity (cumulative  
335 | precipitation for week). However during the early and late monsoon rather show a  
336 | reduction in duration (number of we days for week) (see further details in  
337 | Supplementary Material 2).

338 5.2 Trend analysis in the Koshi Basin

339 | Table 2 provides the descriptive statistics of the Sen's slopes for minT, maxT,  
340 | meanT, and Prec for the 1994-2013 period for the Koshi Basin. The stations located on  
341 | the two sides of the Himalayan range are listed separately. For the southern ones (KO-  
342 | S), we observe that for minT less than half of the stations experience an increasing trend  
343 | and just three are significant with  $p < 0.1$ . In general, the minT on the southern side can  
344 | be defined as stationary ( $+0.003 \text{ }^\circ\text{C a}^+ \text{y}^{-1}$ ). Conversely, the maxT shows a decidedly  
345 | non-stationary condition. All stations present an increasing trend, and even six of the ten  
346 | are on the significant rise with at least  $p < 0.1$ . The mean trend is  $+0.060 \text{ }^\circ\text{C a}^+ \text{y}^{-1}$  ( $p <$   
347 |  $0.10$ ). Similarly, the meanT shows a substantial increase. Also in this case, six of the ten  
348 | stations are on the significant rise with at least  $p < 0.1$ . The mean trend is  $+0.029 \text{ }^\circ\text{C a}^+$   
349 |  $\text{y}^{-1}$  ( $p < 0.10$ ). In regards to Prec, we observe that on the KO-S, 14 of the 19 stations  
350 | present a downward trend. Among them, eight decrease significantly with at least  $p <$   
351 |  $0.1$ . The mean trend is  $-11.1 \text{ mm a}^+ \text{y}^{-1}$ , i.e., we observe a decreasing of 15% (222 mm)  
352 | of precipitation fallen in the basin during the 1994-2013 period (1527 mm on average).

353 The two stations located on the northern ridge (KO-N) show a singularly slight sig-  
354 nificant rise for minT ( $\pm 0.034 \text{ }^\circ\text{C a}^{-1}\text{y}^{-1}$ ,  $p < 0.10$  on average) and for maxT ( $\pm 0.039 \text{ }^\circ\text{C}$   
355  $\text{a}^{-1}\text{y}^{-1}$ ,  $p < 0.10$  on average), recording a consequent mean increase of meanT equal to  
356  $\pm 0.037 \text{ }^\circ\text{C a}^{-1}\text{y}^{-1}$ ,  $p < 0.05$ . As for Prec, we observe that on the KO-N both stations  
357 maintain stationary conditions ( $-0.1 \text{ mm a}^{-1}\text{y}^{-1}$ ).

358 Table 3 provides the descriptive statistics of the Sen's slopes on a seasonal base. The  
359 stations analyzed here are the same as those considered in Table 2. We begin our  
360 description with PYRAMID, already analyzed in detail in Figure 4. We confirm with  
361 this seasonal grouping that the main and significant increases of minT, maxT, and  
362 meanT are completely concentrated during the post-monsoon period (e.g.,  $\pm 0.124 \text{ }^\circ\text{C a}^{-1}$   
363  $\text{y}^{-1}$ ,  $p < 0.01$  for meanT). The pre-monsoon period experienced a slighter and not  
364 significant increase (e.g.,  $\pm 0.035 \text{ }^\circ\text{C y}^{-1}$ ,  $p > 0.1$  for meanT). In general, during the  
365 monsoon period, T is much more stationary for all three variables (e.g.,  $\pm 0.015 \text{ }^\circ\text{C y}^{-1}$ ,  $p$   
366  $> 0.1$  for meanT). Considering the other KO-S stations, the main increasing and  
367 significant trends of meanT occurred during the pre-monsoon ( $\pm 0.043 \text{ }^\circ\text{C a}^{-1}\text{y}^{-1}$ ) and  
368 post-monsoon ( $\pm 0.030 \text{ }^\circ\text{C a}^{-1}\text{y}^{-1}$ ) season, while the increase during the monsoon is  
369 slighter ( $\pm 0.020 \text{ }^\circ\text{C a}^{-1}\text{y}^{-1}$ ). The KO-N stations confirm that the main increasing trend of  
370 meanT occurred outside the monsoon period that is stationary ( $+0.013 \text{ }^\circ\text{C a}^{-1}\text{y}^{-1}$ ).

371 As for Prec, PYRAMID and the other KO-S stations show that the magnitude of the  
372 Sen's slopes is higher during the monsoon season ( $-9.3 \text{ mm a}^{-1}\text{y}^{-1}$  and  $-8.6 \text{ mm a}^{-1}\text{y}^{-1}$ ,  
373 respectively), when precipitation is more abundant. The relatively low snowfall phase of  
374 monsoon Prec at PYRAMID (as specified above) makes the decreasing trend observed  
375 during the summer more robust than the annual one as devoid of ~~possible—the~~  
376 undervaluation of snowfall, although slight as demonstrated above ( $3\pm 1\%$ ). The  
377 northern stations show slight significant decreasing Prec during the winter ( $-3.3 \text{ mm a}^{-1}$   
378  $\text{y}^{-1}$ ,  $p < 0.05$ ).

### 379 5.3 Lapse rates in the southern Koshi Basin

#### 380 5.3.1 Air temperature gradient

381 This study, aiming to create a connection between the climate drivers and cryosphere  
382 in the Koshi Basin, which presents the highest altitudinal gradient of the world (77 to  
383 8848 m a.s.l.), offers a unique opportunity to calculate T and Prec lapse rates before  
384 analyzing their spatial trends. It is worth noting that the T lapse rate is one of the most  
385 important variables for modeling meltwater runoff from a glacierized basin using the T-  
386 index method (Hock, 2005; Immerzeel et al., 2014). It is also an important variable for  
387 determining the form of Prec and its distribution characteristics (e.g., Hock, 2005).  
388 Figure 5a-5b presents the lapse rate of the annual meanT in the KO Basin (Nepal) along  
389 the altitudinal range of well over 7000 m (865 to 7986 m a.s.l.). We found an altitudinal  
390 gradient of  $-0.60 \text{ }^\circ\text{C (100 m)}^{-1}$  on the annual scale with a linear trend ( $r^2 = 0.98$ ,  $p <$   
391  $0.001$ ). It is known that up to altitudes of approximately 8-17 km a.s.l. in the lower  
392 regions of the atmosphere, T decreases with altitude at a fairly uniform rate (Washington

393 | and Parkinson, 2005). ~~Kattel and Yao (2013) recently found a lower annual lapse rate~~  
394 | ~~for the overall CH S, but until 4000 m a.s.l.:  $-0.52\text{ }^{\circ}\text{C}(100\text{ m})^{-1}$ .~~

395 | Considering that the lapse rate is mainly affected by the moisture content of the air  
396 | (Washington and Parkinson, 2005), we ~~also~~ calculated the seasonal gradients (not  
397 | shown here). We found a dry lapse rate of  $-0.65\text{ }^{\circ}\text{C}(100\text{ m})^{-1}$  ( $r^2 = 0.99$ ,  $p < 0.001$ )  
398 | during the pre-monsoon season when AWS1 registers a mean relative humidity of 62%.  
399 | A saturated lapse rate during the monsoon season is  $-0.57\text{ }^{\circ}\text{C}(100\text{ m})^{-1}$  ( $r^2 = 0.99$ ,  $p <$   
400 |  $0.001$ ) with a mean relative humidity of 96%. During the post-monsoon period, we  
401 | found a lapse rate equal to that registered during the monsoon:  $-0.57(100\text{ m})^{-1}$  ( $r^2 =$   
402 |  $0.98$ ,  $p < 0.001$ ) even if the relative humidity is decidedly lower in these months (44%).  
403 | Kattel ~~et al. (2013) and Yao (2013)~~ explain this anomalous low post-monsoon lapse rate  
404 | as the effect of strong radiative cooling in winter.

### 405 | 5.3.2 Precipitation gradient

406 | ~~The relationship of Prec with elevation helps in As for Prec, its relationship with~~  
407 | ~~elevation helps in~~ providing a realistic assessment of water resources and hydrological  
408 | modeling of mountainous regions (Barros et al., 2004). In recent years, the spatial  
409 | variability of Prec has received attention because the mass losses of the Himalayan  
410 | glaciers can be explained with an increased variability in the monsoon system (e.g., Yao  
411 | et al., 2012; Thakuri et al., 2014). ~~Some previous studies of the Himalayas have~~  
412 | ~~considered orographic effects on Prec (Singh and Kumar, 1997; Ichiyonagi et al., 2007).~~  
413 | ~~Ichiyonagi et al. (2007), using all available Prec stations operated by DHM, of which~~  
414 | ~~5% of stations are located over 2500 m and just one station is over 4000 m a.s.l.,~~  
415 | ~~observed that in the CH S region, the annual Prec increases with altitude below 2000 m~~  
416 | ~~a.s.l. and decreases for elevations ranging between 2000 and 3500 m a.s.l., but with no~~  
417 | ~~significant gradient. A broad picture of the relationship between Prec and topography in~~  
418 | ~~the Himalayas can be derived from the precipitation radar onboard the Tropical Rainfall~~  
419 | ~~Measuring Mission (TRMM). Some authors found an increasing trend with elevation~~  
420 | ~~characterized by two distinct maxima along two elevation bands (950 and 2100 m~~  
421 | ~~a.s.l.). The second maximum is much higher than the first, and it is located along the~~  
422 | ~~Lesser Himalayas. Over these elevations, the annual distribution follows an~~  
423 | ~~approximate exponentially decreasing trend (Bookhagen and Burbank, 2006).~~

424 | Figure 5ab shows the altitudinal gradient for the total annual Prec in the Koshi Basin.  
425 | We observe a clear rise in Prec with elevation until approximately 2500 m a.s.l.,  
426 | corresponding to the Tarke Ghyang station (code 1058), registering an annual mean of  
427 | 3669 mm (mean for the 2004-2012 period). A linear approximation ( $r = 0.83$ ,  $p < 0.001$ )  
428 | provides a rate of  $+1.16\text{ mm m}^{-1}$ . At higher elevations, we observe an exponential  
429 | decrease ( $ae^{bx}$ , with  $a = 21168\text{ mm m}^{-1}$  and  $b = -9\text{ }10^{-4}\text{ m}^{-1}$ , where  $x$  is the elevation  
430 | expressed as m a.s.l.) until observing a minimum of 132 mm (years 2009 and 2013) for  
431 | the Kala Patthar station (AWS4) at 5600 m a.s.l., although, as specified above, at these  
432 | altitudes the contribution of winter snowfall could be slightly underestimated. The

Codice campo modificato

433 changing point between the two gradients can be reasonably assumed at approximately  
434 2500 m a.s.l., considering that the stations here present the highest interannual  
435 variability, belonging in this way, depending on the year, to the linear increase or to the  
436 exponential decrease. The clear outlier along the linear gradient is the Num Station  
437 (1301) located at 1497 m a.s.l., which recorded 4608 mm of precipitation. This station  
438 has been excluded for the linear approximation because, as reported by Montgomery  
439 and Stolar (2006), the station is located in the Arun Valley, which acts as a conduit for  
440 northward transport of monsoonal precipitation. The result is that local precipitation  
441 within the gorge of the Arun River is several times greater than in surrounding areas.

442 Some previous studies of the Himalayas have considered orographic effects on Prec  
443 (Singh and Kumar, 1997; Ichiyangi et al., 2007). Ichiyangi et al. (2007), using all  
444 available Prec stations operated by DHM, of which < 5% of stations are located over  
445 2500 m and just one station is over 4000 m a.s.l., observed that in the CH-S region, the  
446 annual Prec increases with altitude below 2000 m a.s.l. and decreases for elevations  
447 ranging between 2000 and 3500 m a.s.l., but with no significant gradient. A broad  
448 picture of the relationship between Prec and topography in the Himalayas can be  
449 derived from the precipitation radar onboard the Tropical Rainfall Measuring Mission  
450 (TRMM). Some authors found an increasing trend with elevation characterized by two  
451 distinct maxima along two elevation bands (950 and 2100 m a.s.l.). The second  
452 maximum is much higher than the first, and it is located along the Lesser Himalayas.  
453 Over these elevations, the annual distribution follows an approximate exponentially  
454 decreasing trend (Bookhagen and Burbank, 2006).

455 Physically, we can interpret the Prec gradient of Fig. 5a considering that when the  
456 humid air masses coming from the Bay of Bengal collide with the orographic barrier,  
457 heavy convections induce huge quantity of rain below 2500 m a.s.l.. The topographic  
458 barrier of the Himalayan mountain range causes the mechanical lift of the humid air, the  
459 cooling of the air column, the condensation and the consequent rainfall. The further  
460 increase in relief induces a depletion of the moisture content resulting in a severe  
461 reduction of Prec at higher altitudes. Our study, based on ground stations, confirms the  
462 general Prec gradient detected with the TRMM microwave observations, even if we did  
463 not identified a marked double maximum Prec peak as observed generally for the whole  
464 central Himalaya by Bookhagen and Burbank, 2006. In fact these author report for our  
465 specific case study (profiles 14 and 15 of their Fig.1(b)) a single step increase in relief  
466 associated with a single Prec maximum.

467 5.4 Spatial distribution of air temperature and precipitation trends in the Koshi Basin

468 Figure 6 presents the spatial distribution of the Sen's slopes in the Koshi Basin for  
469 minT (Fig. 6a), maxT (Fig. 6b), meanT (Fig. 6c), and Prec (Fig. 6d) during the 1994-  
470 2013 period. The relevant data are reported in Table 2. The Chainpur (East) station  
471 shows T trends in contrast with the other stations (see also Table 2); therefore, we  
472 consider this station as a local anomaly and do not discuss it further in the following  
473 sections.

474 In regards to minT, we observe an overall stationary condition in KO-S, as noted  
475 above. The only two stations showing a significant increasing trend are both located at  
476 East. The high elevation stations (PYRAMID and both those located on the north ridge)  
477 differ from the general pattern of the southern basin by showing a significant increasing  
478 trend. Even for maxT, we observe a higher increase in the southeastern basin. The  
479 central and western parts of the KO-S seem to be more stationary. PYRAMID follows  
480 this stationary pattern, while the northern stations (KO-N) show large and significant  
481 increases. As a consequence, meanT shows increasing trends for all the Koshi Basin,  
482 especially on the southeast and northern sides.

483 The decrease of precipitation in the southern Koshi Basin presents a quite  
484 homogeneous pattern from which the highly elevated PYRAMID is not excluded. The  
485 pattern is different on the north ridge, where it is stationary.

## 486 6 Discussion

### 487 6.1 Temperature trends of the Koshi Basin compared to the regional pattern

488 The trend analysis carried out in this study for the last two decades in KO-S shows  
489 full consistency with the pattern of change (shown in the following) occurring in these  
490 regions over the last three decades in terms of a higher increase in maxT (+0.060 °C y<sup>-1</sup>)  
491 than in minT (+0.003 °C y<sup>-1</sup>), a seasonal pattern (more pronounced during the pre- and  
492 post-monsoon months), and the magnitudes of the trends (e.g., the meanT trend is  
493 +0.030 °C y<sup>-1</sup>). Therefore, at low elevations of KO-S, we observe an acceleration of  
494 warming in the recent years compared to the rate of change reported by Kattel and Yao  
495 (2013) and Shrestha et al. (1999) in the previous decades.

496 At regional level, Kattel and Yao (2013) analyzed the annual minT, maxT, and  
497 meanT trends from stations ranging from 1304 m to 2566 m a.s.l. in CH-S (correspond-  
498 ing to all stations in Nepal) during the 1980–2009 period. They found that the magni-  
499 tude of warming is higher for maxT ( $\pm 0.065$  °C a<sup>-1</sup>y<sup>-1</sup>), while minT ( $\pm 0.011$  °C a<sup>-1</sup>y<sup>-1</sup>)  
500 exhibits larger variability, such as positive, negative or no change; meanT was found to  
501 increase at an intermediate rate of  $\pm 0.038$  °C a<sup>-1</sup>y<sup>-1</sup>. These authors extended some time  
502 series and confirmed the findings of Shrestha et al. (1999) that, analyzing the 1971-1994  
503 period, found a maxT increase of  $\pm 0.059$  °C a<sup>-1</sup>y<sup>-1</sup> for all of Nepal. Furthermore, warm-  
504 ing in the winter was more pronounced compared to other seasons in both studies.  
505 These results are consistent with the pattern reported in WH (e.g., Bhutiyani et al.,  
506 2007; Shekhar et al., 2010), in EH, and in the rest of India (e.g., Pal and Al-Tabbaa,  
507 2010) for the last three decades.

508 ~~The trend analysis carried out in this study for the last two decades in KO-S shows~~  
509 ~~full consistency with the pattern of change occurring in these regions over the last three~~  
510 ~~decades in terms of a higher increase in maxT (0.060 °C a<sup>-1</sup>) than in minT (0.003 °C a<sup>-1</sup>)~~  
511 ~~, a seasonal pattern (more pronounced during the pre- and post-monsoon months), and~~  
512 ~~the magnitudes of the trends (e.g., the meanT trend is +0.030 °C a<sup>-1</sup>). Therefore, at low~~  
513 ~~elevations of KO-S, we observe an acceleration of warming in the recent years com-~~

514 ~~pared to the rate of change reported by Kattel and Yao (2013) and Shrestha et al. (1999)~~  
515 ~~in the previous decades.~~

516 ~~The trend analysis carried out in this study for the last two decades in KO-N agrees~~  
517 ~~with the regional studies (shown in the following) in regards to both the considerable~~  
518 ~~increase of minT (+0.034 °C y<sup>-1</sup>) and the seasonal consistency of trends, related to all~~  
519 ~~three T variables, outside the monsoon months. However, we observe that in recent~~  
520 ~~years, maxT is increasing more than the rest of the TP (+0.039 °C y<sup>-1</sup>). In general we~~  
521 ~~observed an increase of meanT (0.037 °C y<sup>-1</sup>) comparable to that reported by Yang et al.~~  
522 ~~(2012) (0.031 °C y<sup>-1</sup>) in the 1971–2007 period.~~

523 ~~At regional level, Different conditions have been observed~~ on the TP, ~~where~~ the  
524 warming of minT is more prominent than that of maxT (e.g., Liu et al., 2006; Liu et al.,  
525 2009). In particular, for stations above 2000 m a.s.l. during the 1961–2003 period, Liu  
526 et al. (2006) found that minT trends were consistently greater (+0.041 °C a<sup>-1</sup>y<sup>-1</sup>) than  
527 those of maxT (+0.018 °C a<sup>-1</sup>y<sup>-1</sup>), especially in the winter and spring months. Yang et al.  
528 (2012), focusing their analysis on CH-N (which corresponds to the southern TP) in a  
529 more recent period (1971–2007), showed a significant increase of  $\pm 0.031$  °C a<sup>-1</sup>y<sup>-1</sup> for  
530 meanT. Yang et al. (2006) analyzed five stations located in a more limited area of CH-  
531 N: the northern side of Mt. Everest (therefore, including the two stations also considered  
532 in this study) from 1971 to 2004. The warming is observed to be influenced more mark-  
533 edly by the minT increase.

534 ~~The trend analysis carried out in this study for KO-N over the last two decades~~  
535 ~~agrees with these studies in regards to both the considerable increase of minT (0.034 °C~~  
536 ~~a<sup>-1</sup>) and the seasonal consistency of trends, related to all three T variables, outside the~~  
537 ~~monsoon months. However, we observe that in recent years, maxT is increasing more~~  
538 ~~than the rest of the TP (0.039 °C a<sup>-1</sup>). In general we observed an increase of meanT~~  
539 ~~(0.037 °C a<sup>-1</sup>) comparable to that reported by Yang et al. (2012) (0.031 °C a<sup>-1</sup>) in the~~  
540 ~~1971–2007 period.~~

541 ~~With all these regional studies, Summarizing~~ PYRAMID shares the higher T trends  
542 outside the monsoon period. However, in contrast with studies located south of the  
543 Himalayan ridge, which observed a prevalence of maxT increase, PYRAMID experi-  
544 enced a consistent minT increase ( $\pm 0.072$  °C a<sup>-1</sup>y<sup>-1</sup> for PYRAMID vs  $\pm 0.003$  °C a<sup>-1</sup>y<sup>-1</sup>  
545 for KO-S stations), while the maxT increase is decidedly weaker ( $\pm 0.009$  °C a<sup>-1</sup>y<sup>-1</sup> for  
546 PYRAMID vs  $\pm 0.060$  °C a<sup>-1</sup>y<sup>-1</sup> for KO-S stations). The remarkable minT trend of  
547 PYRAMID is higher, but more similar to the pattern of change commonly described on  
548 the TP, in particular in CH-N, and also in this study ( $\pm 0.072$  °C a<sup>-1</sup>y<sup>-1</sup> for PYRAMID vs  
549  $\pm 0.034$  °C a<sup>-1</sup>y<sup>-1</sup> for KO-N stations), while the maxT increase is weaker ( $\pm 0.009$  °C a<sup>-1</sup>y<sup>-1</sup>  
550  $\pm 1$  for PYRAMID vs  $\pm 0.039$  °C a<sup>-1</sup>y<sup>-1</sup> for KO-N stations).

## 551 6.2 Elevation dependency of temperature trends

552 Figure 7 shows T trends in the KO Basin for minT, meanT, and maxT relative to the  
553 elevation during the 1994–2013 period. No linear pattern emerges. However, we can

554 observe the minT trend of the three stations located at higher altitude (PYRAMID and  
555 KO-N stations), which increases more than that of the lower stations (Fig. 7a, see also  
556 Table 2). Reviewing the most recent studies in the surroundings, we found that they are  
557 quite exclusively located on CH-N. These studies often show contradictory elevation  
558 dependencies (Rangwala and Miller, 2012). A recent study by You et al. (2010) did not  
559 find any significant elevation dependency in the warming rates of meanT between 1961  
560 and 2005. However, considering mostly the same stations, Liu et al. (2009) found that  
561 the warming rates for minT were greater at higher elevations. Observations from CH-S  
562 are much rarer. Shrestha et al. (1999) found elevation dependency in the rate at which  
563 maxT were increasing in the Nepali Himalayas (CH-S), with higher rates at higher  
564 elevations, but this study exclusively considered stations under 3000 m a.s.l.

565 Furthermore we did not find for the Koshi Basin any significant elevation  
566 dependency in the weakening rates of Prec.

### 567 6.3 Precipitation trends of the Koshi Basin compared to the regional pattern

568 As will be detailed in the following, different from the north side of Mt. Everest and  
569 from the general TP, we confirm the general monsoon weakening in the KO-S,  
570 observing a substantial Prec decrease of 15% (-11.1 mm y<sup>-1</sup>, -222 mm), but that is not  
571 significant for all stations. At PYRAMID, the annual loss is relatively comparable with  
572 that of the KO-S (-13.7 mm y<sup>-1</sup>, -273 mm), but at these high elevations, as we observed  
573 in Table 2, the weather is much more drier (449 and 1527 mm, respectively). Therefore,  
574 the fractional loss is more than 3 times (-52%) that of the KO-S. Considering that the  
575 decreasing trend observed during the summer is more robust than the annual one (see  
576 above), the fractional loss of Prec during the monsoon is -47%, which means that  
577 currently, on average, the precipitation at PYRAMID is the half of what it was twenty  
578 years ago.

579 At regional level, Turner and Annamalai (2012), using the all-India rainfall data  
580 based on a weighted mean of 306 stations, observed a negative precipitation trend since  
581 the 1950s in South Asia. According to Yao et al. (2012), using the Global Precipitation  
582 Climatology Project (GPCP) data, there is strong evidence that precipitation from 1979  
583 to 2010 decreased even in the Himalayas. In eastern CH-S, where the Koshi Basin is  
584 located, they estimated a loss of 173 mm, showing a real decreasing trend starting from  
585 the early 1990s (mean value between grid 9 and 11 in Fig. S18 of their paper).

586 On the TP, the observed pattern of change is opposite that of the monsoon weakening  
587 described by the authors cited above. Liu et al. (2010) described an increase in  
588 precipitation in CH-N for the period of the 1980s to 2008. Su et al. (2006) described a  
589 marked precipitation increase in the Yangtze River Basin (eastern CH-N). In a similar  
590 way to the T analysis, Yang et al. (2006) considered 5 stations located on the northern  
591 side of Mt. Everest (therefore, including the two stations also considered in this study)  
592 from 1971 to 2004 and observed an increasing, but not significant Prec trend. The  
593 higher stationarity we observed is confirmed since 1971 for the two KO-N stations

594 considered in this study.

595 ~~Different from the north side of Mt. Everest and from the general TP, we confirm the~~  
596 ~~general monsoon weakening in the KO-S, observing a substantial Prec decrease of 15%~~  
597 ~~(11.1 mm a<sup>-1</sup>, 222 mm), but that is not significant for all stations. At PYRAMID, the~~  
598 ~~annual loss is relatively comparable with that of the KO-S (13.7 mm a<sup>-1</sup>, 273 mm), but~~  
599 ~~at these high elevations, as we observed in Table 2, the weather is much more drier (449~~  
600 ~~and 1527 mm, respectively). Therefore, the fractional loss is more than 3 times (52%)~~  
601 ~~that of the KO-S. Considering that the decreasing trend observed during the summer is~~  
602 ~~more robust than the annual one (see above), the fractional loss of Prec during the~~  
603 ~~monsoon is 47%, which means that currently, on average, the precipitation at~~  
604 ~~PYRAMID is the half of what it was twenty years ago.~~

#### 605 6.4 Mechanisms responsible for temperature warming and precipitation weakening

606 According to Rangwala and Miller (2012), there are a number of mechanisms that  
607 can cause enhanced warming rates at high elevation, and they often have strong  
608 seasonal dependency. These mechanisms arise from either elevation based differential  
609 changes in climate drivers, such as snow cover, clouds, specific humidity, aerosols, and  
610 soil moisture, or differential sensitivities of surface warming to changes in these drivers  
611 at different elevations. This study does not aim to either realize a comprehensive review  
612 or to demonstrate the causes that could have led to the climate change pattern observed  
613 at PYRAMID, but our intent here is just to note the recent hypotheses advanced in the  
614 literature that fit with our observations for the region of investigation.

615 Snow/ice albedo is one of the strongest feedbacks in the climate system (Rangwala  
616 and Miller, 2012). Increases in minT are possible if decreases in snow cover are  
617 accompanied by increases in soil moisture and surface humidity, which can facilitate a  
618 greater diurnal retention of the daytime solar energy in the land surface and amplify the  
619 longwave heating of the land surface at night (Rangwala et al., 2012). For the Tibetan  
620 Plateau, Rikiishi and Nakasato (2006) found that the length of the snow cover season  
621 declined at all elevations between 1966 and 2001. Moreover, minT can be enhanced by  
622 nighttime increases in cloud cover. However, assessing changes in clouds and  
623 quantifying cloud feedbacks will remain challenging in the near term. For the Tibetan  
624 Plateau, Duan and Wu (2006) found that low level nocturnal cloud cover increased over  
625 the TP between 1961 and 2003 and that these increases explain part of the observed  
626 increases in minT.

627 The maxT increase observed here during April ( $p < 0.05$  in 2011, Fig. 4b) fits with  
628 the warming reported by Pal and Al-Tabbaa (2010) which observed that within the pre-  
629 monsoon season only April shows significant changes in maxT in all Indian regions and  
630 WH (1901-2003 period). According to Ramanathan et al. (2007), Gautam et al. (2010)  
631 argued that the observed warming during the pre-monsoon period (April-June) can be  
632 ascribed not only to the global greenhouse warming, but also to the solar radiation ab-  
633 sorption caused by the large amount of aerosol (mineral dust mixed with other carbona-

634 ceous material) transported over the Gangetic-Himalayan region. As recently reported  
635 by Marinoni et al. (2013), April represents the month for which the transport of absorb-  
636 ing carbonaceous aerosol (i.e. black carbon) is maximized in our region of investigation  
637 (Khumbu Valley). At this regards Putero et al. (2013) show evidences for a possible in-  
638 fluence of open fire occurrence in South Asia particular abundant during this period of  
639 the year. However the significant decreasing of maxT observed in May ( $p < 0.05$ ) and  
640 the slight significant decreasing during the monsoon months from June to August ( $p <$   
641  $0.10$ ) appear to deviate from the scenario proposed for April. In this respect it should be  
642 kept in mind that the radioactive dynamical interactions of aerosol with the monsoon  
643 cycle are extremely complex and different processes can interact with each other. As an  
644 instance, as reported by Qian et al. (2011), the deposition of absorbing aerosol on snow  
645 and the snow albedo feedback processes can play a prominent role in Himalayas and TP  
646 inducing large radioactive flux changes and surface temperature perturbation.

647 Recent studies associate the precipitation decrease over India during the second half  
648 of 20<sup>th</sup> century (e.g., Ramanathan et al., 2005; Lau and Kim, 2006) to the significant  
649 tropospheric warming over the tropical area from the Indian Ocean to the western  
650 Pacific (e.g., Wu, 2005), while westerlies are strengthening (Zhao et al., 2012). Other  
651 authors (e.g., Bollasina et al., 2011) attribute the monsoon weakening to human-  
652 influenced aerosol emissions. In fact an increase of aerosols over South Asia has been  
653 well documented (Ramanathan et al., 2005; Lau and Kim, 2006) and climate model  
654 experiments suggest that sulfate aerosol may significantly reduce monsoon precipitation  
655 (Mitchell and Johns, 1997). Despite a historical weakening of the monsoon circulation,  
656 most studies project an increase of the seasonal monsoon rainfall under global warming.  
657 At this regards Levy II et al., 2013 find that the dramatic emission reductions (35%–  
658 80%) in anthropogenic aerosols and their precursors projected by Representative  
659 Concentration Pathway (RCP) 4.5 (Moss et al., 2010) result an increasing trend by the  
660 second half of the 21st century in South Asia and in particular over the Himalaya  
661 (Palazzi et al., 2013).

## 662 6.5 Linking climate change patterns observed at high elevation with glacier responses

### 663 6.5.1 *Impact of temperature increase*

664 Air temperature and precipitation are the two factors most commonly related to  
665 glacier fluctuations. However, there still exists a seasonal gap in order to explain the  
666 shrinking of summer accumulation-type glaciers (typical of CH) due to large  
667 temperature increases observed in the region during winter (Ueno and Aryal, 2008), as  
668 is the case for the south slopes of Mt. Everest. Furthermore, in this study we noted a  
669 slightly significant decline in summer maxT and stationary meanT. The real increase of  
670 T has been observed for minT, but given the mean elevation of glaciers (5695 m a.s.l. in  
671 1992) and the mean elevation range of glacier fronts (4568-4817 m a.s.l. in 1992, mean  
672 4817 m a.s.l., 249 m of standard deviation –sd-) (Thakuri et al., 2014), this increase for  
673 minT can be most likely considered ineffective for melting processes, since T is still less

674 than 0 °C. This inference can be ascertained analyzing Figure 8, created in order to link  
675 temperature increases and altitudinal glacier distribution (data from Thakuri et al.,  
676 2014). The 0 °C isotherms, corresponding to the mean monthly minT and maxT, are  
677 plotted for 1994 and 2013. The elevation of each 0 °C isotherm is calculated according  
678 to the accurate lapse rates computation carried out in this study and the observed  
679 monthly T trends. We can note that in 1994 the 0 °C isotherm for minT reached the  
680 elevation band characterizing the glacier fronts only from June to September. However,  
681 | twenty years later, the upward of the 0 °C isotherm is modest (+92 m) during these  
682 months, compared to the huge but ineffective rise for melting processes (downstream  
683 | from the glacier fronts) of December-November (even +854 m). The maxT has  
684 obviously a greater potential impact on glaciers. In fact the 0 °C isotherm for of all  
685 months except January and February crosses the elevation bands within which the  
686 glacier fronts are located ever since 1994. In this regard we observe that only April  
687 | (+224 m), December (+212 m), and November (+160 m) experienced an upward of the  
688 0 °C isotherm able to enhance the melting processes, but only close to the glaciers  
689 fronts. We therefore point out that the impact caused by the increased temperature  
690 occurring in April most likely plays an important role not only in relation to this case  
691 study, but also at the level of the Himalayan range. In fact, as mentioned above, Pal and  
692 Al-Tabbaa (2010), observed that within the pre-monsoon season, only April showed  
693 significant changes in maxT in all Indian regions and WH (1901-2003 period).

#### 694 6.5.2 Impact of precipitation decrease

695  
696 As regards the precipitation, in this study we noted a strong and significant  
697 decreasing Prec trend for all months, corresponding to a fractional loss of 47% during  
698 the monsoon season which indicates that, on average, the precipitation at PYRAMID is  
699 currently half of what it was twenty years ago. This climate change pattern confirms and  
700 clarifies the observation of Thakuri et al. (2014), who noted that the southern Mt.  
701 Everest glaciers experienced a shrinkage acceleration over the last twenty years (1992-  
702 2011), as underlined by an upward shift of SLA with a velocity almost three times  
703 greater than the previous period (1962-1992). The authors, without the support of  
704 climatic data, proposed the hypothesis that Mt. Everest glaciers are shrinking faster  
705 since the early 1990s mainly as a result of a weakening of precipitation over the last  
706 decades. In fact they observed a double upward shift in the SLA of the largest glaciers  
707 (south-oriented and with a higher altitude accumulation zone): a clear signal of a  
708 significant decrease in accumulation. Wagnon et al. (2013) have recently reached the  
709 same conclusion, but also in this case without the support of any climatic studies. Bolch  
710 et al. (2011) and Nuimura et al. (2012) registered a higher mass loss rate during the last  
711 decade (2000–2010).

712 Furthermore Quincey et al. (2009) and Peters et al. (2010) observed lower glacier  
713 flow velocity in the region over the last decades. Many studies highlight how the  
714 present condition of ice stagnation of glaciers in the Mt Everest region, and in general

715 in CH-S, is attributable to low flow velocity generated by generally negative mass  
716 balances (Bolch et al., 2008; Quincey et al., 2009; Scherler et al., 2011). Our  
717 observations allow attributing the lower glacier flow velocity to lower accumulation due  
718 to weaker precipitation, which can thus be considered the main climatic factor driving  
719 the current ice stagnation of tongues. In this regard we need to keep in mind that  
720 changes in velocity are among the main triggers for the formation of supraglacial and  
721 proglacial lakes (Salerno et al., 2012; Quincey et al., 2009), which we know to be  
722 susceptible to GLOFs.

### 723 *6.5.3 Trend analysis of annual probability of snowfall*

724 Figure 9 analyses how the changes observed for the meanT at PYRAMID have  
725 affected the probability of snowfall on total cumulated annual precipitation in the last  
726 twenty years. The increase of meanT observed outside the monsoon period, when the  
727 precipitation is almost completely composed by snow (Fig. 2), brought a significant  
728 decrease of solid phase ( $+0.7\% \text{ a}^{-1}\text{y}^{-1}$ ,  $p < 0.05$ ). Extending this analysis to the elevation  
729 bands characterizing the glaciers distribution (see Fig. 8), through the temperature lapse  
730 rate calculated here, we observe that at the level of the mean glaciers (5695 m a.s.l.) the  
731 probability of snowfall is stationary ( $+0.04\% \text{ a}^{-1}\text{y}^{-1}$ ), while it decreases at the mean  
732 elevation of SLAs (5345 m a.s.l. in 1992, Thakuri et al., 2014), but not significantly ( $-$   
733  $0.38\% \text{ a}^{-1}\text{y}^{-1}$ ,  $p > 0.1$ ). The reduction becomes significant at lower altitudes. In  
734 particular, at the mean elevation of glacier fronts (4817 m a.s.l.) the probability of  
735 snowfall is  $-0.56\% \text{ a}^{-1}\text{y}^{-1}$  ( $p < 0.05$ ), i.e. at these altitudes the probability of snow on  
736 annual base is currently 11% ( $p < 0.05$ ) less than twenty years ago. We can conclude  
737 this analysis summarizing that a significant change in precipitation phase has occurred  
738 close to the terminal portions of glaciers, corresponding broadly to the glaciers ablation  
739 zones (around 10%,  $p < 0.5$ ), while the lower temperature of the upper glaciers zones  
740 has so far guaranteed a stationary condition.

### 741 **Conclusion**

742 Most relevant studies on temperature trends were conducted on the Tibetan Plateau,  
743 the Indian subcontinent (including the WH) and the Upper Indus Basin, while studies  
744 on the mountainous regions along the southern slope of the central Himalayas in Nepal  
745 (CH-S) are limited. Although Shrestha et al. (1999) analyzed the maximum temperature  
746 trends over Nepal during the period 1971–1994, studies on recent temperature trends  
747 over CH-S are still lacking and, before this study, completely absent as regards high  
748 elevation. This paper addresses seasonal variability of minimum, maximum, and mean  
749 temperatures and precipitation at high elevation on the southern slopes of Mt. Everest.  
750 Moreover, we complete this analysis with data from all the existing weather stations  
751 located on both sides of the Himalayan range (Koshi Basin) for the 1994-2013 period,  
752 during which a rapider glacier mass loss occurred.

753 At high elevation on the southern slopes of Mt. Everest, we observed the following:

- 754 1) The main increases in air temperature are almost completely concentrated during  
755 the post-monsoon months. The pre-monsoon period experienced a slighter and  
756 insignificant increase, while the monsoon season is generally stationary. This  
757 seasonal temperature change pattern is shared with the entire Koshi Basin, and it  
758 is also observed in the regional studies related to the northern and southern  
759 slopes of the Himalayan range. Surprisingly, ~~at high elevation~~above 5000 m  
760 a.s.l. the maximum temperature decreases significantly in May and slightly  
761 during the monsoon months from June to August.
- 762 2) The minimum temperature increased much more than the maximum  
763 temperature. This remarkable minimum temperature trend is more similar to the  
764 pattern of change commonly described on the Tibetan Plateau and confirmed in  
765 this study in the northern Koshi Basin. However, this trend is in contrast with  
766 studies located south of the Himalayan ridge. As proved by this study, the  
767 southern Koshi Basin experienced a prevalence of maximum temperature  
768 increases. No linear pattern emerges in the elevation dependency of temperature  
769 trends. We only observed higher minimum temperature trends at higher  
770 altitudes.
- 771 3) The total annual precipitation has considerably decreased. The annual rate of  
772 decrease ~~at high elevation~~above 5000 m a.s.l. is similar to the one -at lower  
773 altitudes on the southern side of the Koshi Basin, but the drier conditions of this  
774 remote environment make the fractional loss relatively more consistent. The  
775 precipitation at high elevation during the monsoon period is currently half of  
776 what it was twenty years ago. These observations confirm the monsoon  
777 weakening observed by previous studies in India and even in the Himalayas  
778 since the early 1980s. As opposed to the northern side of the Koshi Basin that  
779 shows in this study certain stability, as positive or stationary trends have been  
780 observed by previous studies on the TP and more specifically in northern central  
781 Himalaya.
- 782 4) There is a significantly lower probability of snowfall in the glaciers ablation  
783 zones, while the lower temperature of the upper glaciers zones have so far  
784 guaranteed a stationary condition.

785 In general, this study contributes to change the perspective on how the climatic  
786 driver (temperature vs. precipitation) led the glacier responses in the last twenty years.  
787 ~~to a change perspective related to the climatic driver (temperature vs. precipitation) led~~  
788 ~~the glacier responses in the last twenty years.~~

789 Without demonstrating the causes that could have led to the climate change pattern  
790 observed at the PYRAMID, we simply note the recent literature on hypotheses that  
791 accord with our observations. ~~for the case study.~~

792 In conclusion, we have here observed that weather stations at low elevations are not  
793 able to suitably describe the climate changes occurring ~~at high altitudes~~above 5000 m  
794 a.s.l. and thus correctly interpret the impact observed on the cryosphere. This

795 consideration stresses the great importance of long-term ground measurements at high  
796 elevation.

#### 797 **Author contributions**

798 G.T., Y.M. and E.V. designed research; F.S. performed research; F.S., N.G., S.T., G.V.  
799 and E.R. analyzed data; F.S., N.G., E.R. and G.T. wrote the paper. P.C., P.S., N.G. and  
800 G.A. data quality check.

#### 801 **Acknowledgements**

802 This work was supported by the MIUR through Ev-K2-CNR/SHARE and CNR-  
803 DTA/NEXTDATA project within the framework of the Ev-K2-CNR and Nepal  
804 Academy of Science and Technology (NAST). Sudeep Thakuri is recipient of the IPCC  
805 Scholarship Award under the collaboration between the IPCC Scholarship Programme  
806 and the Prince Albert II of Monaco Foundation's Young Researchers Scholarships  
807 Initiative.

#### 808 **References**

- 809 [Abebe, A., Solomatine, D., and Venneker, R.: Application of adaptive fuzzy rule based](#)  
810 [models for reconstruction of missing precipitation events, Hydrolog. Sci. J., 45, 425–](#)  
811 [436, doi:10.1080/02626660009492339, 2000.](#)
- 812 [Abudu, S., Bawazir, A. S., and King, J. P.: Infilling missing daily evapotranspiration](#)  
813 [data using neural networks, J. Irrig. Drain. E-asc, 136, 317–325,](#)  
814 [doi:10.1061/\(ASCE\)IR.1943-4774.0000197, 2010.](#)
- 815 [Amatya, L. K., Cuccillato, E., Haack, B., Shadie, P., Sattar, N., Bajracharya, B.,](#)  
816 [Shrestha, B. Caroli, P., Panzeri, D., Basani, M., Schommer, B., Flury, B. Salerno, F.,](#)  
817 [and Manfredi, E. C.: Improving communication for management of social-ecological](#)  
818 [systems in high mountain areas: Development of methodologies and tools – The](#)  
819 [HKKH Partnership Project, Mt. Res. Dev., 30, 69-79, doi:10.1659/MRD-JOURNAL-](#)  
820 [D-09-00084.1, 2010.](#)
- 821 [Bajracharya B., Uddin, K., Chettri, N., Shrestha, B., and Siddiqui, S. A.: Understanding](#)  
822 [land cover change using a harmonized classification system in the Himalayas: A case](#)  
823 [study from Sagarmatha National Park, Nepal, Mt. Res. Dev., 30, 143–156, doi:](#)  
824 [10.1659/MRD-JOURNAL-D-09-00044.1, 2010.](#)
- 825 [Barros, A. P., Kim, G., Williams, E., and Nesbitt, S .W.: Probing orographic controls in](#)  
826 [the Himalayas during the monsoon using satellite imagery, Nat. Hazards Earth Syst.](#)  
827 [Sci. 4, 29–51, doi:10.5194/nhess-4-29-2004, 2004.](#)
- 828 [Benn, D. I., Bolch, T., Hands, K., Gulley, J., Luckman, A., Nicholson, L. I., Quincey,](#)  
829 [D., Thompson, S., Toumi, R., and Wiseman, S.: Response of debris-covered glaciers](#)  
830 [in the Mount Everest region to recent warming, and implications for outburst flood](#)  
831 [hazards, Earth-Sci. Rev., 114, 156–174, doi:10.1016/j.earscirev.2012.03.008, 2012.](#)

832 [Bertolani L., Bollasina, M., and Tartari, G.: Recent biannual variability of](#)  
833 [meteorological features in the Eastern Highland Himalayas, \*Geophys. Res. Lett.\*, 27,](#)  
834 [2185-2188, doi:10.1029/1999GL011198, 2000.](#)

835 [Bhutiyani, M. R., Kale, V. S., and Pawar, N. J.: Long-term trends in maximum,](#)  
836 [minimum and mean annual air temperatures across the Northwestern Himalaya](#)  
837 [during the twentieth century, \*Climatic Change\*, 85, 159–177, doi:10.1007/s10584-](#)  
838 [006-9196-1, 2007.](#)

839 [Bocchiola, D. and Diolaiuti, G.: Evidence of climate change within the Adamello](#)  
840 [Glacier of Italy, \*Theor. Appl. Climatol.\*, 100, 351–369, doi:10.1007/s00704-009-](#)  
841 [0186-x, 2010.](#)

842 [Bolch T., Buchroithner, M., Pieczonka, T., and Kunert, A.: Planimetric and volumetric](#)  
843 [glacier changes in the Khumbu Himal, Nepal, since 1962 using Corona, Landsat TM](#)  
844 [and ASTER data, \*J. Glaciol.\*, 54, 592–600, doi: 0.3189/002214308786570782, 2008.](#)

845 [Bolch T., Kulkarni, A., Kääb, A., Huggel, C., Paul, F., Cogley, J. G., Frey, H., Kargel, J.](#)  
846 [S., Fujita, K., Scheel, M., Bajracharya, S., and Stoffel, M.: The state and fate of](#)  
847 [Himalayan glaciers, \*Science\*, 336, 310-314, doi: 10.1126/science.1215828, 2012.](#)

848 [Bolch T., Pieczonka, T., and Benn, D.I.: Multi-decadal mass loss of glaciers in the](#)  
849 [Everest area \(Nepal Himalaya\) derived from stereo imagery, \*The Cryosphere\*, 5,](#)  
850 [349–358, doi:10.5194/tc-5-349-2011, 2011.](#)

851 [Bollasina, M. A., Ming, Y., and Ramaswamy, V.: Anthropogenic aerosols and the](#)  
852 [weakening of the south Asian summer monsoon, \*Science\*, 334, 502-505,](#)  
853 [doi:10.1126/science.1204994, 2011.](#)

854 [Bookhagen, B. and Burbank, D. W.: Topography, relief, and TRMM-derived rainfall](#)  
855 [variations along the Himalaya, \*Geophys. Res. Lett.\*, 33, L08405,](#)  
856 [doi:10.1029/2006GL026037, 2006.](#)

857 [Carraro, E., Guyennon, N., Hamilton, D., Valsecchi, L., Manfredi, E. C., Viviano, G.,](#)  
858 [Salerno, F., Tartari, G., and Copetti, D.: Coupling high-resolution measurements to a](#)  
859 [three-dimensional lake model to assess the spatial and temporal dynamics of the](#)  
860 [cyanobacterium \*Planktothrix rubescens\* in a medium-sized lake, \*Hydrobiologia\*, 698](#)  
861 [\(1\), 77-95. doi:10.1007/s10750-012-1096-y, 2012.](#)

862 [Carraro, E., Guyennon, N., Viviano, G., Manfredi, E. C., Valsecchi, L., Salerno, F.,](#)  
863 [Tartari, G., and Copetti, D.: Impact of Global and Local Pressures on the Ecology of](#)  
864 [a Medium-Sized Pre-Alpine Lake, in \*Models of the Ecological Hierarchy\*, edited by:](#)  
865 [Jordan, F., and Jorgensen, S. E., Elsevier B.V., pp. 259-274, doi:10.1016/B978-0-](#)  
866 [444-59396-2.00016-X, 2012b.](#)

867 [Coulibaly, P. and Evora, N.: Comparison of neural network methods for infilling](#)  
868 [missing daily weather records, \*J. Hydrol.\*, 341, 27–41,](#)  
869 [doi:10.1016/j.jhydrol.2007.04.020, 2007.](#)

870 [Déqué, M.: Frequency of precipitation and temperature extremes over France in an](#)  
871 [anthropogenic scenario: model results and statistical correction according to](#)  
872 [observed values, \*Global Planet. Change\*, 57, 16–26,](#)  
873 [doi:10.1016/j.gloplacha.2006.11.030, 2007.](#)

874 [Duan, A. and Wu, G.: Change of cloud amount and the climate warming on the Tibetan](#)  
875 [Plateau, \*Geophys. Res. Lett.\*, 33, L22704, doi:10.1029/2006GL027946, 2006.](#)  
876 [Dytham, C.: \*Choosing and Using Statistics: A Biologist's Guide\*, John Wiley & Sons,](#)  
877 [2011.](#)  
878 [Fujita, K., and Sakai, A.: Modelling runoff from a Himalayan debris-covered glacier,](#)  
879 [Hydrol. Earth Syst. Sci., 18, 2679–2694, doi:10.5194/hess-18-2679-2014, 2014.](#)  
880 [Fujita, K., Sakai, A., Takenaka, S., Nuimura, T., Surazakov, A. B., Sawagaki, T., and](#)  
881 [Yamanokuchi T.: Potential flood volume of Himalayan glacial lakes, \*Nat. Hazards\*](#)  
882 [Earth Syst. Sci., 13, 1827–1839, doi:10.5194/nhessd-1-15-2013, 2013.](#)  
883 [Ganguly, N. D. and Iyer, K. N.: Long-term variations of surface air temperature during](#)  
884 [summer in India, \*Int. J. Climatol.\*, 29, 735–746, doi:10.1002/joc.1748, 2009.](#)  
885 [Gardelle, J., Arnaud, Y., and Berthier, E.: Contrasted evolution of glacial lakes along the](#)  
886 [Hindu Kush Himalaya mountain range between 1990 and 2009, \*Global Planet.\*](#)  
887 [Change, 75, 47-55, doi:10.1016/j.gloplacha.2010.10.003, 2011.](#)  
888 [Gautam, R., Hsu, N. C. and Lau, K. M.: Premonsoon aerosol characterization and](#)  
889 [radiative effects over the Indo-Gangetic plains: implications for regional climate](#)  
890 [warming, \*J. Geophys. Res.\*, 115, D17208, doi:10.1029/2010JD013819, 2010.](#)  
891 [Gerstengarbe, F. W. and Werner, P. C.: Estimation of the beginning and end of recurrent](#)  
892 [events within a climate regime, \*Clim. Res.\*, 11, 97-107, 1999.](#)  
893 [Guyennon, N., Romano, E., Portoghese, I., Salerno, F., Calmanti, S., Petrangeli, A. B.,](#)  
894 [Tartari, G., and Copetti, D.: Benefits from using combined dynamical-statistical](#)  
895 [downscaling approaches – lessons from a case study in the Mediterranean region,](#)  
896 [Hydrol. Earth Syst. Sc., 17, 705–720, doi:10.5194/hess-17-705-2013, 2013.](#)  
897 [Hock, R.: Glacier melt: a review of processes and their modeling, \*Prog. Phys. Geog.\*,](#)  
898 [29, 362-391, doi:10.1191/0309133305pp453ra, 2005.](#)  
899 [Ichiyanagi, K., Yamanaka, M. D., Muraji, Y., and Vaidya, B. K.: Precipitation in Nepal](#)  
900 [between 1987 and 1996, \*Int. J. Climatol.\*, 27, 1753–1762, doi:10.1002/joc.1492,](#)  
901 [2007.](#)  
902 [Immerzeel, W. W., Petersen, L., Ragetti, S., and Pellicciotti, F.: The importance of](#)  
903 [observed gradients of air temperature and precipitation for modeling runoff from a](#)  
904 [glacierized watershed in the Nepal Himalayas, \*Water Resour. Res.\*, 50,](#)  
905 [doi:10.1002/2013WR014506, 2014.](#)  
906 [James, A. L. and Oldenburg, C. M.: Linear and Monte Carlo uncertainty analysis for](#)  
907 [subsurface contaminant transport simulation, \*Water Resour. Res.\*, 33, 2495–2508,](#)  
908 [doi:10.1029/97WR01925, 1997.](#)  
909 [Kattel, D. B. and Yao, T.: Recent temperature trends at mountain stations on the](#)  
910 [southern slope of the central Himalayas, \*J. Earth Syst. Sci.\*, 122, 215–227, doi:](#)  
911 [10.1007/s12040-012-0257-8, 2013.](#)  
912 [Kattel, D. B., Yao, T., Yang, K., Tian, L., Yang, G. and Joswiak, D.: Temperature lapse](#)  
913 [rate in complex mountain terrain on the southern slope of the central Himalayas,](#)  
914 [Theor. Appl. Climatol., 113, 671-682, doi:10.1007/s00704-012-0816-6, 2013.](#)  
915 [Kendall, M.G.: \*Rank Correlation Methods\*, Oxford University Press, New York, 1975.](#)

916 [Kivekas, N., Sun, J., Zhan, M., Kerminen, V. M., Hyvarinen, A., Komppula, M.,](#)  
917 [Viisanen, Y., Hong, N., Zhang, Y., Kulmala, M., Zhang, X. C., Deli-Geer, and](#)  
918 [Lihavainen, H.: Long term particle size distribution measurements at Mount](#)  
919 [Waliguan, a high-altitude site in inland China, \*Atmos. Chem. Phys.\*, 9, 5461–5474,](#)  
920 [doi:10.5194/acp-9-95461-2009, 2009.](#)

921 [Lami, A., Marchetto, A., Musazzi, S., Salerno, F., Tartari, G., Guilizzoni, P., Rogora, M.,](#)  
922 [and Tartari, G. A.: Chemical and biological response of two small lakes in the](#)  
923 [Khumbu Valley, Himalayas \(Nepal\) to short-term variability and climatic change as](#)  
924 [detected by long-term monitoring and paleolimnological methods, \*Hydrobiologia\*,](#)  
925 [648, 189-205, doi:10.1007/s10750-010-0262-3, 2010.](#)

926 [Lau, K.-M., and Kim, K.-M.: Observational relationships between aerosol and Asian](#)  
927 [monsoon rainfall, and circulation, \*Geophys. Res. Lett.\*, 33, L21810,](#)  
928 [doi: 10.1029/2006GL027546, 2006.](#)

929 [Lavagnini, I., Badocco, D., Pastore, P., and Magno, F.: Theil-Sen nonparametric regres-](#)  
930 [sion technique on univariate calibration, inverse regression and detection limits, \*Ta-\*](#)  
931 [lanta](#), 87, 180-188, doi:10.1016/j.talanta.2011.09.059, 2011.

932 [Levy II, H., L. W., Horowitz, M. D., Schwarzkopf, Y., Ming, J. C., Golaz, V., Naik, and](#)  
933 [Ramaswamy, V.: The roles of aerosol direct and indirect effects in past and future](#)  
934 [climate change, \*J. Geophys. Res.\*, 118, 1–12, doi:10.1002/jgrd.50192, 2013.](#)

935 [Liu, J., Yang, B., and Qin, C.: Tree-ring based annual precipitation reconstruction since](#)  
936 [AD 1480 in south central Tibet, \*Quatern. Int.\*, 236, 75-81,](#)  
937 [doi:10.1016/j.quaint.2010.03.020, 2010.](#)

938 [Liu, K., Cheng, Z., Yan, L., and Yin, Z.: Elevation dependency of recent and future min-](#)  
939 [imum surface air temperature trends in the Tibetan Plateau and its surroundings,](#)  
940 [Global Planet. Change, 68, 164–174, doi:10.1016/j.gloplacha.2009.03.017, 2009.](#)

941 [Liu, X. D., and Chen, B. D.: Climatic warming in the Tibetan Plateau during recent](#)  
942 [decades, \*Int. J. Climatol.\*, 20, 1729–1742, doi:10.1002/1097-](#)  
943 [0088\(20001130\)20:14<1729::AID-JOC556>3.0.CO;2-Y, 2000.](#)

944 [Liu, X.D., Yin, Z. Y., Shao, X., and Qin, N.: Temporal trends and variability of daily](#)  
945 [maximum and minimum, extreme temperature events, and growing season length](#)  
946 [over the eastern and central Tibetan Plateau during 1961–2003, \*J. Geophys. Res.\*,](#)  
947 [111, D19, doi:10.1029/2005JD006915, 2006.](#)

948 [Manfredi, E. C., Flury, B., Viviano, G., Thakuri, S., Khanal, S. N., Jha, P. K., Maskey,](#)  
949 [R. K., Kayastha, R. B., Kafle, K. R., Bhochhibhoya, S., Ghimire, N. P., Shrestha, B.](#)  
950 [B., Chaudhary, G., Giannino, F., Carteni, F., Mazzoleni, S., and Salerno, F.: Solid](#)  
951 [waste and water quality management models for Sagarmatha National Park and](#)  
952 [Buffer Zone, Nepal: implementation of a participatory modeling framework, \*Mt.\*](#)  
953 [Res. Dev.](#), 30, 127-142, doi:10.1659/MRD-JOURNAL-D-10-00028.1, 2010.

954 [Marinoni, A., Cristofanelli, P., Laj, P., Putero, D., Calzolari, F., Landi, T. C., Vuillermoz,](#)  
955 [E., Maione, M., and Bonasoni, P.: High black carbon and ozone concentrations](#)  
956 [during pollution transport in the Himalayas: Five years of continuous observations at](#)  
957 [NCO-Prec global GAW station, \*J. Environ. Sci.\*, 25, 1618–1625, doi:10.1016/S1001-](#)

958 [0742\(12\)60242-3, 2013.](#)  
959 [Menne, M. J., Durre, I., Vose, R. S., Gleason, B. E., and Houston, T. G.: An overview of](#)  
960 [the Global Historical Climatology Network—daily database, \*J. Atmos. Oceanic\*](#)  
961 [Technol., 29, 897–910, 2012.](#)  
962 [Mitchell, J. F. B. and Johns, T. C.: On the modification of global warming by sulphate](#)  
963 [aerosols. \*J. Climate\*, 10, 245-267, 1997.](#)  
964 [Montgomery, D. R. and Stolar, D. B.: Reconsidering Himalayan river anticlines,](#)  
965 [Geomorphology, 82, 4–15, doi:10.1016/j.geomorph.2005.08.021, 2006.](#)  
966 [Moss, R. H., et al.: The next generation of scenarios for climate change research and](#)  
967 [assessment, \*Nature\*, 463, 747–756, doi:10.1038/nature08823, 2010.](#)  
968 [Nuimura, T., Fujita, K., Yamaguchi, S., and Sharma, R. R.: Elevation changes of](#)  
969 [glaciers revealed by multitemporal digital elevation models calibrated by GPS survey](#)  
970 [in the Khumbu region, Nepal Himalaya, 1992–2008, \*J. Glaciol.\*, 58, 648–656, doi:](#)  
971 [10.3189/2012JoG11J061, 2012.](#)  
972 [Pal, I. and Al-Tabbaa, A.: Long-term changes and variability of monthly extreme tem-](#)  
973 [peratures in India, \*Theor. Appl. Climatol.\*, 100, 45–56, doi:10.1007/s00704-009-](#)  
974 [0167-0, 2010.](#)  
975 [Palazzi, E., von Hardenberg, J., and Provenzale, A.: Precipitation in the Hindu-Kush](#)  
976 [Karakoram Himalaya: Observations and future scenarios, \*J. Geophys. Res.\*, 118, 85-](#)  
977 [100, doi: 10.1029/2012JD018697, 2013.](#)  
978 [Pepin, N. C. and Lundquist, J. D.: Temperature trends at high elevations: patterns across](#)  
979 [the globe, \*Geophys. Res. Lett.\*, 35, doi:10.1029/2008GL034026, 2008.](#)  
980 [Peters, J., Bolch, T., Buchroithner, M. F., and Bäbler, M.: Glacier Surface Velocities in](#)  
981 [the Mount Everest Area/Nepal using ASTER and Ikonos imagery, \*Proceeding of 10th\*](#)  
982 [International Symposium on High Mountain Remote Sensing Cartography,](#)  
983 [Kathmandu, Nepal, 313-320, 2010.](#)  
984 [Putero, D., T. C., Landi, P., Cristofanelli, A., Marinoni, P., Laj, R., Duchi, F., Calzolari,](#)  
985 [G. P., Verza and P. Bonasoni, Influence of open vegetation fires on black carbon and](#)  
986 [ozone variability in the southern Himalayas \(NCO-P, 5079 m a.s.l.\), \*Environ. Pollut.\*,](#)  
987 [184, 597-604, doi: 10.1016/j.envpol.2013.09.035, 2013.](#)  
988 [Qian, Y., Flanner, M., Leung, L., and Wang, W.: Sensitivity studies on the impacts of](#)  
989 [Tibetan plateau snowpack pollution on the Asian hydrological cycle and monsoon](#)  
990 [climate, \*Atmos. Chem. Phys.\*, 11, 1929–1948, doi:10.5194/acp-11-1929-2011, 2011.](#)  
991 [Quincey, D. J., Luckman, A., and Benn, D.: Quantification of Everest region glacier ve-](#)  
992 [locities between 1992 and 2002, using satellite radar interferometry and feature](#)  
993 [tracking, \*J. Glaciol.\*, 55, 596-606, doi: 10.3189/002214309789470987, 2009.](#)  
994 [Ramanathan, V., Chung, C., Kim, D., Bettge, T., Buja, L., Kiehl, J. T., Washington, W.](#)  
995 [M., Fu, Q., Sikka, D. R., and Wild, M.: Atmospheric brown clouds: Impacts on South](#)  
996 [Asian climate and hydrological cycle. \*Proc. Natl. Acad. Sci. U.S.A.\*, 102, 5326- 5333,](#)  
997 [doi: 10.1073/pnas.0500656102, 2005.](#)  
998 [Ramanathan, V., Li, F., Ramana, M. V., Praveen, P. S., Kim, D., Corrigan, C. E.,](#)  
999 [Nguyen, H., Stone, E. A., Schauer, J. J., Carmichael, G. R., Adhikary, B., and Yoon,](#)

1000 [S. C.: Atmospheric brown clouds: Hemispherical and regional variations in long-](#)  
1001 [range transport, absorption, and radiative forcing, J. Geophys. Res., 112, D22,](#)  
1002 [doi:10.1029/2006JD008124, 2007.](#)

1003 [Rangwala, I. and Miller, J. R.: Climate change in mountains: a review of elevation-](#)  
1004 [dependent warming and its possible causes, Climatic Change, 114, 527–547,](#)  
1005 [doi:10.1007/s10584-012-0419-3, 2012.](#)

1006 [Rangwala, I., Barsugli, J., Cozzetto, K., Neff, J., and Prairie, J.: Mid-21st century](#)  
1007 [projections in temperature extremes in the southern Colorado Rocky Mountains from](#)  
1008 [regional climate models, Clim Dyn., 39, 1823-1840, doi:10.1007/s00382- 011-1282-](#)  
1009 [z, 2012.](#)

1010 [Rikiishi, K. and Nakasato, H.: Height dependence of the tendency for reduction in](#)  
1011 [seasonal snow cover in the Himalaya and the Tibetan Plateau region, 1966–2001,](#)  
1012 [Ann. Glaciol., 43, 369–377, doi: http://dx.doi.org/10.3189/172756406781811989,](#)  
1013 [2006.](#)

1014 [Salerno, F., Buraschi, E., Bruccoleri, G., Tartari, G., and Smiraglia, C.: Glacier surface-](#)  
1015 [area changes in Sagarmatha National Park, Nepal, in the second half of the 20th cen-](#)  
1016 [tury, by comparison of historical maps, J. Glaciol., 54, 738-752, 2008.](#)

1017 [Salerno, F., Cuccillato, E., Caroli, P., Bajracharya, B., Manfredi, E. C., Viviano, G.,](#)  
1018 [Thakuri, S., Flury, B., Basani, M., Giannino, F., and Panzeri, D.: Experience with a](#)  
1019 [hard and soft participatory modeling framework for social ecological system man-](#)  
1020 [agement in Mount Everest \(Nepal\) and K2 \(Pakistan\) protected areas, Mt. Res. Dev.,](#)  
1021 [30, 80-93, 2010a.](#)

1022 [Salerno, F., Gambelli, S., Viviano, G., Thakuri, S., Guyennon, N., D’Agata, C.,](#)  
1023 [Diolaiuti, G., Smiraglia, C., Stefani, F., Bochiola, D., and Tartari, G.: High alpine](#)  
1024 [ponds shift upwards as average temperature increase: A case study of the Ortles-](#)  
1025 [Cevedale mountain group \(Southern alps, Italy\) over the last 50 years, Global Planet.](#)  
1026 [Change, doi: 10.1016/j.gloplacha.2014.06.003, 2014.](#)

1027 [Salerno, F., Thakuri, S., D’Agata, C., Smiraglia, C., Manfredi, E. C., Viviano, G., and](#)  
1028 [Tartari, G.: Glacial lake distribution in the Mount Everest region: Uncertainty of](#)  
1029 [measurement and conditions of formation, Global Planet. Change, 92-93, 30-39,](#)  
1030 [doi:10.1016/j.gloplacha.2012.04.001, 2012.](#)

1031 [Salerno, F., Viviano, G., Mangredi, E. C., Caroli, P., Thakuri, S., and Tartari, G.: Multi-](#)  
1032 [ple Carrying Capacities from a management-oriented perspective to operationalize](#)  
1033 [sustainable tourism in protected area, J. Environ. Manage., 128, 116-125,](#)  
1034 [doi:10.1016/j.jenvman.2013.04.043, 2013.](#)

1035 [Salerno, F., Viviano, G., Thakuri, S., Flury, B., Maskey, R. K., Khanal, S. N., Bhujju, D.,](#)  
1036 [Carrer, M., Bhochohibhoya, S., Melis, M. T., Giannino, F., Staiano, A., Carteni, F.,](#)  
1037 [Mazzoleni, S., Cogo, A., Sapkota, A., Shrestha, S., Pandey, R. K., and Manfredi, E.](#)  
1038 [C.: Energy, forest, and indoor air pollution models for Sagarmatha National Park and](#)  
1039 [Buffer zone, Nepal: implementation of a participatory modeling framework, Mt. Res.](#)  
1040 [Dev., 30, 113–126, 2010b.](#)

1041 [Scherler, D., Bookhagen, B., and Strecker, M. R.: Spatially variable response of Hima-](#)

1042 [layan glaciers to climate change affected by debris cover. \*Nature Geosci.\*, 4, 156–](#)  
1043 [159, doi:10.1038/ngeo1068, 2011.](#)

1044 [Schneider, T.: Analysis of incomplete climate data: Estimation of mean values and](#)  
1045 [covariance matrices and imputation of missing values, \*J. Clim.\*, 14, 853–871,](#)  
1046 [doi:10.1175/1520-0442\(2001\)014<0853:AOICDE>2.0.CO;2, 2001.](#)

1047 [Sellegri, K., Laj, P., Venzac, H., Boulon, J., Picard, D., Villani, P., Bonasoni, P.,](#)  
1048 [Marinoni, A., Cristofanelli, P., and Vuillermoz, E.: Seasonal variations of aerosol size](#)  
1049 [distributions based on long-term measurements at the high altitude Himalayan site of](#)  
1050 [Nepal Climate Observatory—Pyramid \(5079 m\), Nepal, \*Atmos. Chem. Phys.\*, 10,](#)  
1051 [10679–10690, doi:10.5194/acp-10.10679-2010, 2010.](#)

1052 [Sen, P. K.: Estimates of the regression coefficient based on Kendall’s Tau, \*J. Am.\*  
1053 \[Assoc., 63, 1379-1389, doi:10.2307/2285891, 1968.\]\(#\)](#)

1054 [Shekhar, M. S., Chand, H., Kumar, S., Srinivasan, K., and Ganju, A.: Climate-change](#)  
1055 [studies in the western Himalaya, \*Ann. Glaciol.\*, 51, 105-112,](#)  
1056 [doi:10.3189/172756410791386508, 2010.](#)

1057 [Shrestha, A. B., Wake, C. P., Mayewski, P. A., and Dibb, J. E.: Maximum temperature](#)  
1058 [trends in the Himalaya and its vicinity: An analysis based on temperature records](#)  
1059 [from Nepal for the period 1971-94, \*J. Clim.\*, 12, 2775-5561, doi:10.1175/1520-](#)  
1060 [0442\(1999\)012<2775:MTTITH>2.0.CO;2, 1999.](#)

1061 [Singh, P. and Kumar, N.: Effect of orography on precipitation in the western Himalayan](#)  
1062 [region, \*J. Hydrol.\*, 199, 183-206, doi:10.1016/S0022-1694\(96\)03222-2, 1997.](#)

1063 [Su, B. D., Jiang, T., and Jin, W. B.: Recent trends in observed temperature and](#)  
1064 [precipitation extremes in the Yangtze River basin, China, \*Theor. Appl. Climatol.\*, 83,](#)  
1065 [139–151, doi:10.1007/s00704-005-0139-y, 2006.](#)

1066 [Tartari, G., Salerno, F., Buraschi, E., Bruccoleri, G., and Smiraglia, C.: Lake surface](#)  
1067 [area variations in the North-Eastern sector of Sagarmatha National Park \(Nepal\) at](#)  
1068 [the end of the 20th Century by comparison of historical maps, \*J. Limnol.\*, 67, 139-](#)  
1069 [154, doi:10.4081/jlimnol.2008.139, 2008.](#)

1070 [Tartari, G., Verza, P., and Bertolami, L.: Meteorological data at PYRAMID Observatory](#)  
1071 [Laboratory \(Khumbu Valley, Sagarmatha National Park, Nepal\), in \*Limnology of\*](#)  
1072 [high altitude lakes in the Mt. Everest Region \(Nepal\), edited by: Lami, A. and](#)  
1073 [Giussani, G., \*Mem. Ist. Ital. Idrobiol.\*, 57, 23-40, 2002.](#)

1074 [Tartari, G., Vuillermoz, E., Manfredi, E. C., and Toffolon, R.: CEOP High Elevations](#)  
1075 [Initiative, \*GEWEX News, Special Issue\*, 19\(3\), 4-5, 2009.](#)

1076 [Thakuri, S., Salerno, F., Smiraglia, C., Bolch, T., D’Agata, C., Viviano, G., and Tartari,](#)  
1077 [G.: Tracing glacier changes since the 1960s on the south slope of Mt. Everest \(central](#)  
1078 [southern Himalaya\) using optical satellite imagery, \*The Cryosphere\*, 8, 1297-1315,](#)  
1079 [doi:10.5194/tc-8-1297-2014, 2014.](#)

1080 [Themeßl, M. J., Gobiet, A., and Heinrich, G.: Empirical-statistical downscaling and](#)  
1081 [error correction of regional climate models and its impact on the climate change](#)  
1082 [signal, \*Climatic Change\*, 112, 449-468, doi:10.1007/s10584-011-011-0224-4, 2012.](#)

1083 [Turner, A. G. and Annamalai, H.: Climate change and the South Asian summer](#)

1084 [monsoon, Nat. Clim. Change, 2, 587-595, doi:10.1038/nclimate1495, 2012.](#)

1085 [Ueno K. and Aryal, R.: Impact of tropical convective activity on monthly temperature](#)

1086 [variability during non monsoon season in the Nepal Himalayas, J. Geophys. Res.,](#)

1087 [113, D18112, doi:10.1029/2007JD009524, 2008.](#)

1088 [Ueno, K., Endoh, N., Ohata, T., Yabuki, H., Koike, M., and Zhang, Y.: Characteristics of](#)

1089 [precipitation distribution in Tangua, Monsoon, 1993, Bulletin of Glaciological](#)

1090 [Research, 12, 39-46, 1994.](#)

1091 [UNEP \(United Nations Environment Programme\)/WCMC \(World Conservation](#)

1092 [Monitoring Centre\): Sagarmatha National Park, Nepal, in Encyclopedia of Earth,](#)

1093 [edited by: McGinley, M. and Cleveland, C. J., Environmental Information Coalition,](#)

1094 [National Council for Science and the Environment, Washington, DC, 2008.](#)

1095 [Venzac, H., Sellegri, K., Laj, P., Villani, P., Bonasoni, P., Marinoni, A., Cristofanelli, P.,](#)

1096 [Calzolari, F., Fuzzi, S., Decesari, S., Facchini, M. C., Vuillermoz, E., and Verza, G. P.:](#)

1097 [High frequency new particle formation in the Himalayas, Proc. Natl. Acad. Sci.](#)

1098 [USA, 105, 15666-15671, doi:10.1073/pnas.0801355105, 2008.](#)

1099 [Vuille, M.: Climate variability and high altitude temperature and precipitation, in](#)

1100 [Encyclopedia of snow, ice and glaciers, edited by: Singh, V. P. et al., Springer, pp.](#)

1101 [153-156, 2011.](#)

1102 [Wagon, P., Vincent, C., Arnaud, Y., Berthier, E., Vuillermoz, E., Gruber, S., Ménégoz,](#)

1103 [M., Gilbert, A., Dumont, M., Shea, J. M., Stumm, D., and Pokhrel, B. P.: Seasonal](#)

1104 [and annual mass balances of Mera and Pokalde glaciers \(Nepal Himalaya\) since](#)

1105 [2007, The Cryosphere, 7, 1769-1786, doi:10.5194/tc-7-1769-2013, 2013.](#)

1106 [Washington, W. M. and Parkinson, C. L.: An introduction to three-Dimensional Climate](#)

1107 [Modeling, 2<sup>nd</sup> Edition, University Science Books, Sausalito, 2005.](#)

1108 [Wu, B.: Weakening of Indian summer monsoon in recent decades, Adv. Atmos. Sci.](#)

1109 [22\(1\), 21-29, doi:10.1007/BF02930866, 2005.](#)

1110 [Yang J., Tan, C., and Zhang, T.: Spatial and temporal variations in air temperature and](#)

1111 [precipitation in the Chinese Himalayas during the 1971–2007, Int. J. Climatol., 33,](#)

1112 [2622-2632, doi:10.1002/joc.3609, 2012.](#)

1113 [Yang, X., Zhang, Y., Zhang, W., Yan, Y., Wang, Z., Ding, M., and Chu, D.: Climate](#)

1114 [change in Mt. Qomolangma region since 1971, J. Geogr. Sci., 16, 326-336,](#)

1115 [doi:10.1007/s11442-006-0308-7, 2006.](#)

1116 [Yao, T., Thompson, L., Yang, W., Yu, W., Gao, Y., Guo, X., Yang, X., Duan, K., Zhao,](#)

1117 [H., Xu, B., Pu, J., Lu, A., Xiang, Y., Kattel, D. B., and Joswiak, D.: Different glacier](#)

1118 [status with atmospheric circulations in Tibetan Plateau and surroundings, Nat. Clim.](#)

1119 [Change, 2, 663-667, doi:10.1038/nclimate1580, 2012.](#)

1120 [Yasutomi, N., Hamada, A., and Yatagai, A.: Development of a long-term daily gridded](#)

1121 [temperature dataset and its application to rain/snow discrimination of daily](#)

1122 [precipitation, Global Environ. Res., V15N2, 165-172, 2011.](#)

1123 [You, Q., Kang, S., Pepin, N., Flügel, W., Yan, Y., Behrawan, H., and Huang, J.: Rela-](#)

1124 [tionship between temperature trend magnitude, elevation and mean temperature in](#)

1125 [the Tibetan Plateau from homogenized surface stations and reanalysis data, Global](#)

1126 [Planet. Change, 71, 124-133, doi:10.1016/j.gloplacha.2010.01.020, 2010.](#)  
1127 [Zhao, H., Xu, B., Yao, T., Wu, G., Lin, S., Gao, J., and Wang, M.: Deuterium excess](#)  
1128 [record in a southern Tibetan ice core and its potential climatic implications, Clim.](#)  
1129 [Dyn., 38, 1791-1803, doi:10.1007/s00382-011-1161-7, 2012.](#)  
1130  
1131 [Fujita, K., and Sakai, A.: Modelling runoff from a Himalayan debris covered glacier,](#)  
1132 [Hydrol. Earth Syst. Sci., 18, 2679–2694, doi:10.5194/hess-18-2679-2014, 2014.](#)  
1133 [Ueno, K., Endoh, N., Ohata, T., Yabuki, H., Koike, M., and Zhang, Y.: Characteristics of](#)  
1134 [precipitation distribution in Tangula, Monsoon, 1993, Bulletin of Glaciological](#)  
1135 [Research, 12, 39–46, 1994.](#)  
1136 [Abebe, A., Solomatine, D., and Venneker, R.: Application of adaptive fuzzy rule based](#)  
1137 [models for reconstruction of missing precipitation events, Hydrolog. Sci. J., 45, 425–](#)  
1138 [436, doi:10.1080/02626660009492339, 2000.](#)  
1139 [Abudu, S., Bawazir, A. S., and King, J. P.: Infilling missing daily evapotranspiration](#)  
1140 [data using neural networks, J. Irrig. Drain. E-asee, 136, 317–325,](#)  
1141 [doi:10.1061/\(ASCE\)IR.1943-4774.0000197, 2010.](#)  
1142 [Amatya, L. K., Cuccillato, E., Haack, B., Shadie, P., Sattar, N., Bajracharya, B.,](#)  
1143 [Shrestha, B. Caroli, P., Panzeri, D., Basani, M., Schommer, B., Flury, B. Salerno, F.,](#)  
1144 [and Manfredi, E. C.: Improving communication for management of social-ecological](#)  
1145 [systems in high mountain areas: Development of methodologies and tools—The](#)  
1146 [HKKH Partnership Project, Mt. Res. Dev., 30, 69–79, doi:10.1659/MRD-JOURNAL-](#)  
1147 [D-09-00084.1, 2010.](#)  
1148 [Bajracharya B., Uddin, K., Chettri, N., Shrestha, B., and Siddiqui, S. A.: Understanding](#)  
1149 [land cover change using a harmonized classification system in the Himalayas: A case](#)  
1150 [study from Sagarmatha National Park, Nepal, Mt. Res. Dev., 30, 143–156, doi:](#)  
1151 [10.1659/MRD-JOURNAL-D-09-00044.1, 2010.](#)  
1152 [Barros, A. P., Kim, G., Williams, E., and Nesbitt, S. W.: Probing orographic controls in](#)  
1153 [the Himalayas during the monsoon using satellite imagery, Nat. Hazards Earth Syst.](#)  
1154 [Sci. 4, 29–51, doi:10.5194/nhess-4-29-2004, 2004.](#)  
1155 [Benn, D. I., Bolch, T., Hands, K., Gullely, J., Luckman, A., Nicholson, L. I., Quincey,](#)  
1156 [D., Thompson, S., Toumi, R., and Wiseman, S.: Response of debris covered glaciers](#)  
1157 [in the Mount Everest region to recent warming, and implications for outburst flood](#)  
1158 [hazards, Earth Sci. Rev., 114, 156–174, doi:10.1016/j.earseirev.2012.03.008, 2012.](#)  
1159 [Bertolani L., Bollasina, M., and Tartari, G.: Recent biannual variability of](#)  
1160 [meteorological features in the Eastern Highland Himalayas, Geophys. Res. Lett., 27,](#)  
1161 [2185–2188, doi:10.1029/1999GL011198, 2000.](#)  
1162 [Bhutiyani, M. R., Kale, V. S., and Pawar, N. J.: Long term trends in maximum,](#)  
1163 [minimum and mean annual air temperatures across the Northwestern Himalaya](#)  
1164 [during the twentieth century, Climatic Change, 85, 159–177, doi:10.1007/s10584-](#)  
1165 [006-9196-1, 2007.](#)  
1166 [Bocchiola, D. and Diolaiuti, G.: Evidence of climate change within the Adamello](#)  
1167 [Glacier of Italy, Theor. Appl. Climatol., 100, 351–369, doi:10.1007/s00704-009-](#)

1168 ~~0186-x, 2010.~~

1169 ~~Boleh T., Kulkarni, A., Kääh, A., Huggel, C., Paul, F., Cogley, J. G., Frey, H., Kargel, J.~~

1170 ~~S., Fujita, K., Scheel, M., Bajracharya, S., and Stoffel, M.: The state and fate of~~

1171 ~~Himalayan glaciers, *Science*, 336, 310-314, doi: 10.1126/science.1215828, 2012.~~

1172 ~~Boleh T., Buchroithner, M., Pieczonka, T., and Kunert, A.: Planimetric and volumetric~~

1173 ~~glacier changes in the Khumbu Himal, Nepal, since 1962 using Corona, Landsat TM~~

1174 ~~and ASTER data, *J. Glaciol.*, 54, 592-600, doi: 0.3189/002214308786570782, 2008.~~

1175 ~~Boleh T., Pieczonka, T., and Benn, D.I.: Multi-decadal mass loss of glaciers in the~~

1176 ~~Everest area (Nepal Himalaya) derived from stereo imagery, *The Cryosphere*, 5,~~

1177 ~~349-358, doi:10.5194/te-5-349-2011, 2011.~~

1178 ~~Bollasina, M. A., Ming, Y., and Ramaswamy, V.: Anthropogenic aerosols and the~~

1179 ~~weakening of the south Asian summer monsoon, *Science*, 334, 502-505,~~

1180 ~~doi:10.1126/science.1204994, 2011.~~

1181 ~~Bookhagen, B. and Burbank, D. W.: Topography, relief, and TRMM derived rainfall~~

1182 ~~variations along the Himalaya, *Geophys. Res. Lett.*, 33, L08405,~~

1183 ~~doi:10.1029/2006GL026037, 2006.~~

1184 ~~Carraro, E., Guyennon, N., Hamilton, D., Valsecchi, L., Manfredi, E. C., Viviano, G.,~~

1185 ~~Salerno, F., Tartari, G., and Copetti, D.: Coupling high-resolution measurements to a~~

1186 ~~three-dimensional lake model to assess the spatial and temporal dynamics of the~~

1187 ~~cyanobacterium *Planktothrix rubescens* in a medium-sized lake, *Hydrobiologia*, 698~~

1188 ~~(1), 77-95. doi:10.1007/s10750-012-1096-y, 2012.~~

1189 ~~Carraro, E., Guyennon, N., Viviano, G., Manfredi, E. C., Valsecchi, L., Salerno, F.,~~

1190 ~~Tartari, G., and Copetti, D.: Impact of Global and Local Pressures on the Ecology of~~

1191 ~~a Medium-Sized Pre-Alpine Lake, in *Models of the Ecological Hierarchy*, edited by:~~

1192 ~~Jordan, F., and Jorgensen, S. E., Elsevier B.V., pp. 259-274, doi:10.1016/B978-0-~~

1193 ~~444-59396-2.00016-X, 2012b.~~

1194 ~~Coulibaly, P. and Evora, N.: Comparison of neural network methods for infilling~~

1195 ~~missing daily weather records, *J. Hydrol.*, 341, 27-41,~~

1196 ~~doi:10.1016/j.jhydrol.2007.04.020, 2007.~~

1197 ~~Déqué, M.: Frequency of precipitation and temperature extremes over France in an~~

1198 ~~anthropogenic scenario: model results and statistical correction according to~~

1199 ~~observed values, *Global Planet. Change*, 57, 16-26,~~

1200 ~~doi:10.1016/j.gloplacha.2006.11.030, 2007.~~

1201 ~~Duan, A. and Wu, G.: Change of cloud amount and the climate warming on the Tibetan~~

1202 ~~Plateau, *Geophys. Res. Lett.*, 33, L22704, doi:10.1029/2006GL027946, 2006.~~

1203 ~~Dytham, C.: *Choosing and Using Statistics: A Biologist's Guide*, John Wiley & Sons,~~

1204 ~~2011.~~

1205 ~~Fujita, K., Sakai, A., Takenaka, S., Nuimura, T., Surazakov, A. B., Sawagaki, T., and~~

1206 ~~Yamanokuchi T.: Potential flood volume of Himalayan glacial lakes, *Nat. Hazards*~~

1207 ~~*Earth Syst. Sci.*, 13, 1827-1839, doi:10.5194/nhessd-1-15-2013, 2013.~~

1208 ~~Ganguly, N. D. and Iyer, K. N.: Long term variations of surface air temperature during~~

1209 ~~summer in India, *Int. J. Climatol.*, 29, 735-746, doi:10.1002/joc.1748, 2009.~~

1210 Gardelle, J., Arnaud, Y., and Berthier, E.: Contrasted evolution of glacial lakes along the  
1211 Hindu Kush Himalaya mountain range between 1990 and 2009, *Global Planet.*  
1212 *Change*, 75, 47–55, doi:10.1016/j.gloplacha.2010.10.003, 2011.

1213 Gautam, R., Hsu, N. C. and Lau, K. M.: Premonsoon aerosol characterization and  
1214 radiative effects over the Indo-Gangetic plains: implications for regional climate  
1215 warming, *J. Geophys. Res.*, 115, D17208, doi:10.1029/2010JD013819, 2010.

1216 Gerstengarbe, F. W. and Werner, P. C.: Estimation of the beginning and end of recurrent  
1217 events within a climate regime, *Clim. Res.*, 11, 97–107, 1999.

1218 Guyennon, N., Romano, E., Portoghese, I., Salerno, F., Calmanti, S., Petrangeli, A. B.,  
1219 Tartari, G., and Copetti, D.: Benefits from using combined dynamical-statistical  
1220 downscaling approaches—lessons from a case study in the Mediterranean region,  
1221 *Hydrol. Earth Syst. Sc.*, 17, 705–720, doi:10.5194/hess-17-705-2013, 2013.

1222 Hoek, R.: Glacier melt: a review of processes and their modeling, *Prog. Phys. Geog.*,  
1223 29, 362–391, doi:10.1191/0309133305pp453ra, 2005.

1224 Ichiyanagi, K., Yamanaka, M. D., Muraji, Y., and Vaidya, B. K.: Precipitation in Nepal  
1225 between 1987 and 1996, *Int. J. Climatol.*, 27, 1753–1762, doi:10.1002/joc.1492,  
1226 2007.

1227 Immerzeel, W. W., Petersen, L., Ragetti, S., and Pellicciotti, F.: The importance of  
1228 observed gradients of air temperature and precipitation for modeling runoff from a  
1229 glacierized watershed in the Nepal Himalayas, *Water Resour. Res.*, 50,  
1230 doi:10.1002/2013WR014506, 2014.

1231 James, A. L. and Oldenburg, C. M.: Linear and Monte Carlo uncertainty analysis for  
1232 subsurface contaminant transport simulation, *Water Resour. Res.*, 33, 2495–2508,  
1233 doi:10.1029/97WR01925, 1997.

1234 Kattel, D. B. and Yao, T.: Recent temperature trends at mountain stations on the  
1235 southern slope of the central Himalayas, *J. Earth Syst. Sci.*, 122, 215–227, doi:  
1236 10.1007/s12040-012-0257-8, 2013.

1237 Kendall, M.G.: Rank Correlation Methods, Oxford University Press, New York, 1975.

1238 Kivekas, N., Sun, J., Zhan, M., Kerminen, V. M., Hyvarinen, A., Komppula, M.,  
1239 Viisanen, Y., Hong, N., Zhang, Y., Kulmala, M., Zhang, X. C., Deli-Geer, and  
1240 Lihavainen, H.: Long-term particle size distribution measurements at Mount  
1241 Waliguan, a high altitude site in inland China, *Atmos. Chem. Phys.*, 9, 5461–5474,  
1242 doi:10.5194/acp-9-95461-2009, 2009.

1243 Lami, A., Marchetto, A., Musazzi, S., Salerno, F., Tartari, G., Guilizzoni, P., Rogora, M.,  
1244 and Tartari, G. A.: Chemical and biological response of two small lakes in the  
1245 Khumbu Valley, Himalayas (Nepal) to short-term variability and climatic change as  
1246 detected by long-term monitoring and paleolimnological methods, *Hydrobiologia*,  
1247 648, 189–205, doi:10.1007/s10750-010-0262-3, 2010.

1248 Lau, K. M., and Kim, K. M.: Observational relationships between aerosol and Asian  
1249 monsoon rainfall, and circulation, *Geophys. Res. Lett.*, 33, L21810,  
1250 doi: 10.1029/2006GL027546, 2006.

1251 Lavagnini, I., Badoeco, D., Pastore, P., and Magno, F.: Theil-Sen nonparametric regres-

1252 sion technique on univariate calibration, inverse regression and detection limits, *Ta-*  
1253 *lanta*, 87, 180–188, doi:10.1016/j.talanta.2011.09.059, 2011.

1254 Levy H, H., L. W., Horowitz, M. D., Schwarzkopf, Y., Ming, J. C., Golaz, V., Naik, and  
1255 Ramaswamy, V.: The roles of aerosol direct and indirect effects in past and future  
1256 climate change, *J. Geophys. Res.*, 118, 1–12, doi:10.1002/jgrd.50192, 2013.

1257 Liu, J., Yang, B., and Qin, C.: Tree ring based annual precipitation reconstruction since  
1258 AD 1480 in south central Tibet. *Quatern. Int.*, 236, 75–81,  
1259 doi:10.1016/j.quaint.2010.03.020, 2010.

1260 Liu, K., Cheng, Z., Yan, L., and Yin, Z.: Elevation dependency of recent and future min-  
1261 imum surface air temperature trends in the Tibetan Plateau and its surroundings,  
1262 *Global Planet. Change*, 68, 164–174, doi:10.1016/j.gloplacha.2009.03.017, 2009.

1263 Liu, X. D., and Chen, B. D.: Climatic warming in the Tibetan Plateau during recent  
1264 decades, *Int. J. Climatol.*, 20, 1729–1742, doi:10.1002/1097-  
1265 0088(20001130)20:14<1729::AID-JOC556>3.0.CO;2-Y, 2000.

1266 Liu, X.D., Yin, Z. Y., Shao, X., and Qin, N.: Temporal trends and variability of daily  
1267 maximum and minimum, extreme temperature events, and growing season length  
1268 over the eastern and central Tibetan Plateau during 1961–2003, *J. Geophys. Res.*,  
1269 111, D19, doi:10.1029/2005JD006915, 2006.

1270 Manfredi, E. C., Flury, B., Viviano, G., Thakuri, S., Khanal, S. N., Jha, P. K., Maskey,  
1271 R. K., Kayastha, R. B., Kafle, K. R., Bhoehhibhoya, S., Ghimire, N. P., Shrestha, B.  
1272 B., Chaudhary, G., Giannino, F., Carteni, F., Mazzoleni, S., and Salerno, F.: Solid  
1273 waste and water quality management models for Sagarmatha National Park and  
1274 Buffer Zone, Nepal: implementation of a participatory modeling framework, *Mt.*  
1275 *Res. Dev.*, 30, 127–142, doi:10.1659/MRD-JOURNAL-D-10-00028.1, 2010.

1276 Marinoni, A., Cristofanelli, P., Laj, P., Putero, D., Calzolari, F., Landi, T. C., Vuillermoz,  
1277 E., Maione, M., and Bonasoni, P.: High black carbon and ozone concentrations  
1278 during pollution transport in the Himalayas: Five years of continuous observations at  
1279 NCO-Prec global GAW station, *J. Environ. Sci.*, 25, 1618–1625, doi:10.1016/S1001-  
1280 0742(12)60242-3, 2013.

1281 Mitchell, J. F. B. and Johns, T. C.: On the modification of global warming by sulphate  
1282 aerosols, *J. Climate*, 10, 245–267, 1997.

1283 Montgomery, D. R. and Stolar, D. B.: Reconsidering Himalayan river anticlines,  
1284 *Geomorphology*, 82, 4–15, doi:10.1016/j.geomorph.2005.08.021, 2006.

1285 Moss, R. H., et al.: The next generation of scenarios for climate change research and  
1286 assessment, *Nature*, 463, 747–756, doi:10.1038/nature08823, 2010.

1287 Nuimura, T., Fujita, K., Yamaguchi, S., and Sharma, R. R.: Elevation changes of  
1288 glaciers revealed by multitemporal digital elevation models calibrated by GPS survey  
1289 in the Khumbu region, Nepal Himalaya, 1992–2008, *J. Glaciol.*, 58, 648–656, doi:  
1290 10.3189/2012JoG11J061, 2012.

1291 Pal, I. and Al-Tabbaa, A.: Long term changes and variability of monthly extreme tem-  
1292 peratures in India, *Theor. Appl. Climatol.*, 100, 45–56, doi:10.1007/s00704-009-  
1293 0167-0, 2010.

1294 Palazzi, E., von Hardenberg, J., and Provenzale, A.: Precipitation in the Hindu-Kush  
1295 Karakoram Himalaya: Observations and future scenarios, *J. Geophys. Res.*, **118**, 85-  
1296 100, doi: 10.1029/2012JD018697, 2013.

1297 Pepin, N. C. and Lundquist, J. D.: Temperature trends at high elevations: patterns across  
1298 the globe, *Geophys. Res. Lett.*, **35**, doi:10.1029/2008GL034026, 2008.

1299 Peters, J., Bolch, T., Buchroithner, M. F., and Bäßler, M.: Glacier Surface Velocities in  
1300 the Mount Everest Area/Nepal using ASTER and Ikonos imagery, *Proceeding of 10th*  
1301 *International Symposium on High Mountain Remote Sensing Cartography,*  
1302 *Kathmandu, Nepal*, 313-320, 2010.

1303 Putero, D., T. C., Landi, P., Cristofanelli, A., Marinoni, P., Laj, R., Duchi, F., Calzolari,  
1304 G. P., Verza and P. Bonasoni, Influence of open vegetation fires on black carbon and  
1305 ozone variability in the southern Himalayas (NCO-P, 5079 m a.s.l.), *Environ. Pollut.*,  
1306 **184**, 597-604, doi: 10.1016/j.envpol.2013.09.035, 2013.

1307 Qian, Y., Flanner, M., Leung, L., and Wang, W.: Sensitivity studies on the impacts of  
1308 Tibetan plateau snowpack pollution on the Asian hydrological cycle and monsoon  
1309 climate, *Atmos. Chem. Phys.*, **11**, 1929-1948, doi:10.5194/acp-11-1929-2011, 2011.

1310 Quincey, D. J., Luckman, A., and Benn, D.: Quantification of Everest region glacier ve-  
1311 locities between 1992 and 2002, using satellite radar interferometry and feature  
1312 tracking, *J. Glaciol.*, **55**, 596-606, doi: 10.3189/002214309789470987, 2009.

1313 Ramanathan, V., Chung, C., Kim, D., Bettge, T., Buja, L., Kiehl, J. T., Washington, W.  
1314 M., Fu, Q., Sikka, D. R., and Wild, M.: Atmospheric brown clouds: Impacts on South  
1315 Asian climate and hydrological cycle. *Proc. Natl. Acad. Sci. U.S.A.*, **102**, 5326-5333,  
1316 doi: 10.1073/pnas.0500656102, 2005.

1317 Ramanathan, V., Li, F., Ramana, M. V., Praveen, P. S., Kim, D., Corrigan, C. E.,  
1318 Nguyen, H., Stone, E. A., Schauer, J. J., Carmichael, G. R., Adhikary, B., and Yoon,  
1319 S. C.: Atmospheric brown clouds: Hemispherical and regional variations in long-  
1320 range transport, absorption, and radiative forcing, *J. Geophys. Res.*, **112**, D22,  
1321 doi:10.1029/2006JD008124, 2007.

1322 Rangwala, I. and Miller, J. R.: Climate change in mountains: a review of elevation-  
1323 dependent warming and its possible causes, *Climatic Change*, **114**, 527-547,  
1324 doi:10.1007/s10584-012-0419-3, 2012.

1325 Rangwala, I., Barsugli, J., Cozzetto, K., Neff, J., and Prairie, J.: Mid-21st century  
1326 projections in temperature extremes in the southern Colorado Rocky Mountains from  
1327 regional climate models, *Clim Dyn.*, **39**, 1823-1840, doi:10.1007/s00382-011-1282-  
1328 z, 2012.

1329 Rikiishi, K. and Nakasato, H.: Height dependence of the tendency for reduction in  
1330 seasonal snow cover in the Himalaya and the Tibetan Plateau region, 1966-2001,  
1331 *Ann. Glaciol.*, **43**, 369-377, doi: http://dx.doi.org/10.3189/172756406781811989,  
1332 2006.

1333 Salerno, F., Buraschi, E., Bruccoleri, G., Tartari, G., and Smiraglia, C.: Glacier surface-  
1334 area changes in Sagarmatha National Park, Nepal, in the second half of the 20th cen-  
1335 tury, by comparison of historical maps, *J. Glaciol.*, **54**, 738-752, 2008.

1336 ~~Salerno, F., Viviano, G., Mangredi, E. C., Caroli, P., Thakuri, S., and Tartari, G.: Multi-~~  
1337 ~~ple Carrying Capacities from a management oriented perspective to operationalize~~  
1338 ~~sustainable tourism in protected area, J. Environ. Manage., 128, 116-125,~~  
1339 ~~doi:10.1016/j.jenvman.2013.04.043, 2013.~~

1340 ~~Salerno, F., Gambelli, S., Viviano, G., Thakuri, S., Guyennon, N., D'Agata, C.,~~  
1341 ~~Diolaiuti, G., Smiraglia, C., Stefani, F., Boehhiola, D., and Tartari, G.: High alpine~~  
1342 ~~ponds shift upwards as average temperature increase: A case study of the Ortles-~~  
1343 ~~Cevedale mountain group (Southern alps, Italy) over the last 50 years, Global Planet.~~  
1344 ~~Change, doi: 10.1016/j.gloplacha.2014.06.003, 2014.~~

1345 ~~Salerno, F., Thakuri, S., D'Agata, C., Smiraglia, C., Manfredi, E. C., Viviano, G., and~~  
1346 ~~Tartari, G.: Glacial lake distribution in the Mount Everest region: Uncertainty of~~  
1347 ~~measurement and conditions of formation, Global Planet. Change, 92-93, 30-39,~~  
1348 ~~doi:10.1016/j.gloplacha.2012.04.001, 2012.~~

1349 ~~Scherler, D., Bookhagen, B., and Strecker, M.R.: Spatially variable response of Himala-~~  
1350 ~~yan glaciers to climate change affected by debris cover. Nature Geosci., 4, 156-159,~~  
1351 ~~doi:10.1038/ngeo1068, 2011.~~

1352 ~~Schneider, T.: Analysis of incomplete climate data: Estimation of mean values and~~  
1353 ~~covariance matrices and imputation of missing values, J. Clim., 14, 853-871,~~  
1354 ~~doi:10.1175/1520-0442(2001)014<0853:AOICDE>2.0.CO;2, 2001.~~

1355 ~~Sellegri, K., Laj, P., Venzae, H., Boulon, J., Picard, D., Villani, P., Bonasoni, P.,~~  
1356 ~~Marinoni, A., Cristofanelli, P., and Vuillermoz, E.: Seasonal variations of aerosol size~~  
1357 ~~distributions based on long term measurements at the high altitude Himalayan site of~~  
1358 ~~Nepal Climate Observatory Pyramid (5079 m), Nepal, Atmos. Chem. Phys., 10,~~  
1359 ~~10679-10690, doi:10.5194/acp-10.10679-2010, 2010.~~

1360 ~~Sen, P. K.: Estimates of the regression coefficient based on Kendall's Tau, J. Am.~~  
1361 ~~Assoc., 63, 1379-1389, doi:10.2307/2285891, 1968.~~

1362 ~~Shekhar, M. S., Chand, H., Kumar, S., Srinivasan, K., and Ganju, A.: Climate change~~  
1363 ~~studies in the western Himalaya, Ann. Glaciol., 51, 105-112,~~  
1364 ~~doi:10.3189/172756410791386508, 2010.~~

1365 ~~Shrestha, A. B., Wake, C. P., Mayewski, P. A., and Dibb, J. E.: Maximum temperature~~  
1366 ~~trends in the Himalaya and its vicinity: An analysis based on temperature records~~  
1367 ~~from Nepal for the period 1971-94, J. Clim., 12, 2775-5561, doi:10.1175/1520-~~  
1368 ~~0442(1999)012<2775:MTTHTH>2.0.CO;2, 1999.~~

1369 ~~Singh, P. and Kumar, N.: Effect of orography on precipitation in the western Himalayan~~  
1370 ~~region, J. Hydrol., 199, 183-206, doi:10.1016/S0022-1694(96)03222-2, 1997.~~

1371 ~~Su, B. D., Jiang, T., and Jin, W. B.: Recent trends in observed temperature and~~  
1372 ~~precipitation extremes in the Yangtze River basin, China, Theor. Appl. Climatol., 83,~~  
1373 ~~139-151, doi:10.1007/s00704-005-0139-y, 2006.~~

1374 ~~Tartari, G., Vuillermoz, E., Manfredi, E. C., and Toffolon, R.: CEOP High Elevations~~  
1375 ~~Initiative, GEWEX News, Special Issue, 19(3), 4-5, 2009.~~

1376 ~~Tartari, G., Salerno, F., Buraschi, E., Bruccoleri, G., and Smiraglia, C.: Lake surface~~  
1377 ~~area variations in the North-Eastern sector of Sagarmatha National Park (Nepal) at~~

1378 the end of the 20th Century by comparison of historical maps, *J. Limnol.*, 67, 139-  
1379 154, doi:10.4081/jlimnol.2008.139, 2008.

1380 Tartari, G., Verza, P., and Bertolami, L.: Meteorological data at PYRAMID Observatory  
1381 Laboratory (Khumbu Valley, Sagarmatha National Park, Nepal), in *Limnology of*  
1382 *high altitude lakes in the Mt. Everest Region (Nepal)*, edited by: Lami, A. and  
1383 Giussani, G., *Mem. Ist. Ital. Idrobiol.*, 57, 23-40, 2002.

1384 Thakuri, S., Salerno, F., Smiraglia, C., Boleh, T., D'Agata, C., Viviano, G., and Tartari,  
1385 G.: Tracing glacier changes since the 1960s on the south slope of Mt. Everest (central  
1386 southern Himalaya) using optical satellite imagery, *The Cryosphere*, 8, 1297-1315,  
1387 doi:10.5194/te-8-1297-2014, 2014.

1388 Themeßl, M. J., Gobiet, A., and Heinrich, G.: Empirical statistical downscaling and  
1389 error correction of regional climate models and its impact on the climate change  
1390 signal, *Climatic Change*, 112, 449-468, doi:10.1007/s10584-011-0224-4, 2012.

1391 Turner, A. G. and Annamalai, H.: Climate change and the South Asian summer  
1392 monsoon, *Nat. Clim. Change*, 2, 587-595, doi:10.1038/nclimate1495, 2012.

1393 Ueno K. and Aryal, R.: Impact of tropical convective activity on monthly temperature  
1394 variability during non monsoon season in the Nepal Himalayas, *J. Geophys. Res.*,  
1395 113, D18112, doi:10.1029/2007JD009524, 2008.

1396 UNEP (United Nations Environment Programme)/WCMC (World Conservation  
1397 Monitoring Centre): *Sagarmatha National Park, Nepal*, in *Encyclopedia of Earth*,  
1398 edited by: McGinley, M. and Cleveland, C. J., Environmental Information Coalition,  
1399 National Council for Science and the Environment, Washington, DC, 2008.

1400 Venzae, H., Sellegri, K., Laj, P., Villani, P., Bonasoni, P., Marinoni, A., Cristofanelli, P.,  
1401 Calzolari, F., Fuzzi, S., Decesari, S., Facchini, M. C., Vuillermoz, E., and Verza, G. P.:  
1402 High frequency new particle formation in the Himalayas, *Proc. Natl. Acad. Sci.*  
1403 *USA*, 105, 15666-15671, doi:10.1073/pnas.0801355105, 2008.

1404 Vuille, M.: Climate variability and high altitude temperature and precipitation, in  
1405 *Encyclopedia of snow, ice and glaciers*, edited by: Singh, V. P. et al., Springer, pp.  
1406 153-156, 2011.

1407 Wagnon, P., Vincent, C., Arnaud, Y., Berthier, E., Vuillermoz, E., Gruber, S., Ménégoz,  
1408 M., Gilbert, A., Dumont, M., Shea, J. M., Stumm, D., and Pokhrel, B. P.: Seasonal  
1409 and annual mass balances of Mera and Pokalde glaciers (Nepal Himalaya) since  
1410 2007, *The Cryosphere*, 7, 1769-1786, doi:10.5194/te-7-1769-2013, 2013.

1411 Washington, W. M. and Parkinson, C. L.: *An introduction to three-Dimensional Climate*  
1412 *Modeling*, 2<sup>nd</sup> Edition, University Science Books, Sausalito, 2005.

1413 Wu, B.: Weakening of Indian summer monsoon in recent decades, *Adv. Atmos. Sci.*  
1414 22(1), 21-29, doi:10.1007/BF02930866, 2005.

1415 Yang J., Tan, C., and Zhang, T.: Spatial and temporal variations in air temperature and  
1416 precipitation in the Chinese Himalayas during the 1971-2007, *Int. J. Climatol.*, 33,  
1417 2622-2632, doi:10.1002/joc.3609, 2012.

1418 Yang, X., Zhang, Y., Zhang, W., Yan, Y., Wang, Z., Ding, M., and Chu, D.: Climate  
1419 change in Mt. Qomolangma region since 1971, *J. Geogr. Sci.*, 16, 326-336,

1420 ~~doi:10.1007/s11442-006-0308-7, 2006.~~  
1421 ~~Yao, T., Thompson, L., Yang, W., Yu, W., Gao, Y., Guo, X., Yang, X., Duan, K., Zhao,~~  
1422 ~~H., Xu, B., Pu, J., Lu, A., Xiang, Y., Kattel, D. B., and Joswiak, D.: Different glacier~~  
1423 ~~status with atmospheric circulations in Tibetan Plateau and surroundings, *Nat. Clim.*~~  
1424 ~~*Change*, 2, 663–667, doi:10.1038/nclimate1580, 2012.~~  
1425 ~~You, Q., Kang, S., Pepin, N., Flügel, W., Yan, Y., Behrawan, H., and Huang, J.: Rela-~~  
1426 ~~tionship between temperature trend magnitude, elevation and mean temperature in~~  
1427 ~~the Tibetan Plateau from homogenized surface stations and reanalysis data, *Global*~~  
1428 ~~*Planet. Change*, 71, 124–133, doi:10.1016/j.gloplacha.2010.01.020, 2010.~~  
1429 ~~Zhao, H., Xu, B., Yao, T., Wu, G., Lin, S., Gao, J., and Wang, M.: Deuterium excess~~  
1430 ~~record in a southern Tibetan ice core and its potential climatic implications, *Clim-*~~  
1431 ~~*Dyn.*, 38, 1791–1803, doi:10.1007/s00382-011-1161-7, 2012.~~  
1432

1433 *Table 1. List of surface stations belonging to PYRAMID Observatory Laboratory*  
 1434 *network located along the south slopes of Mt. Everest (upper DK Basin).*

| Station ID | Location     | Latitude<br>°N | Longitude<br>°E | Elevation<br>m a.s.l. | Sampling<br>Frequency | Data Availability |            | % of daily missing data |               |
|------------|--------------|----------------|-----------------|-----------------------|-----------------------|-------------------|------------|-------------------------|---------------|
|            |              |                |                 |                       |                       | From              | To         | Air<br>Temperature      | Precipitation |
| AWS3       | Lukla        | 27.70          | 86.72           | 2660                  | 1 hour                | 02/11/2004        | 31/12/2012 | 23                      | 20            |
| AWSN       | Nameche      | 27.80          | 86.71           | 3570                  | 1 hour                | 27/10/2001        | 31/12/2012 | 21                      | 27            |
| AWS2       | Pheriche     | 27.90          | 86.82           | 4260                  | 1 hour                | 25/10/2001        | 31/12/2013 | 15                      | 22            |
| AWS0       | Pyramid      | 27.96          | 86.81           | 5035                  | 2 hours               | 01/01/1994        | 31/12/2005 | 19                      | 16            |
| AWS1       | Pyramid      | 27.96          | 86.81           | 5035                  | 1 hour                | 01/01/2000        | 31/12/2013 | 10                      | 21            |
| ABC        | Pyramid      | 27.96          | 86.82           | 5079                  | 1 hour                | 01/03/2006        | 31/12/2011 | 5                       | 1             |
| AWS4       | Kala Patthar | 27.99          | 86.83           | 5600                  | 10 minutes            | 01/01/2009        | 31/12/2013 | 28                      | 38            |
| AWS5       | South Col    | 27.96          | 86.93           | 7986                  | 10 minutes            | 01/05/2008        | 31/10/2011 | 39                      | 100           |

1435

1436

1437 Table 2. List of ground weather stations located in the Koshi Basin and descriptive  
 1438 statistics of the Sen's slopes for minimum, maximum, and mean air temperatures and  
 1439 total precipitation for the 1994-2012 period. The annual mean air temperature, the total  
 1440 annual mean precipitation, and the percentage of missing daily values is also reported.  
 1441 Level of significance ( $^{\circ}$   $p$ -value = 0.1, \*  $p$ -value = 0.05, \*\*  $p$ -value = 0.01, and \*\*\*  $p$ -  
 1442 value = 0.001).

| ID              | Station Name         | Latitude           | Longitude          | Elevation | Air Temperature    |                |                           |                           |                           | Precipitation |                |                    |
|-----------------|----------------------|--------------------|--------------------|-----------|--------------------|----------------|---------------------------|---------------------------|---------------------------|---------------|----------------|--------------------|
|                 |                      |                    |                    |           | Annual mean        | Missing values | MinT trend                | MaxT Trend                | MeanT trend               | Annual total  | Missing values | Prec trend         |
|                 |                      |                    |                    |           | $^{\circ}\text{C}$ | %              | $^{\circ}\text{C a}^{-1}$ | $^{\circ}\text{C a}^{-1}$ | $^{\circ}\text{C a}^{-1}$ | mm            | %              | $\text{mm a}^{-1}$ |
|                 |                      | $^{\circ}\text{N}$ | $^{\circ}\text{N}$ | m a.s.l.  |                    |                |                           |                           |                           |               |                |                    |
| KO-S<br>(NEPAL) | 1024 DHULIKHEL       | 27.61              | 85.55              | 1552      | 17.1               | 2              | -0.012                    | 0.041                     | 0.026                     | 1191          | 10             | -25.0 *            |
|                 | 1036 PANCHKHAL       | 27.68              | 85.63              | 865       | 21.4               | 10             | 0.038                     | 0.051 *                   | 0.038 $^{\circ}$          | 3669          | 10             | -21.9              |
|                 | 1058 TARKE GHYANG    | 28.00              | 85.55              | 2480      |                    |                |                           |                           |                           | 1369          | 3              | -1.4               |
|                 | 1101 NAGDAHA         | 27.68              | 86.10              | 850       |                    |                |                           |                           |                           | 2484          | 4              | 6.6                |
|                 | 1103 JIRI            | 27.70              | 86.23              | 2003      | 14.4               | 1              | 0.013                     | 0.020                     | 0.014 $^{\circ}$          | 2148          | 2              | 1.3                |
|                 | 1202 CHAURIKARK      | 27.70              | 86.71              | 2619      |                    |                |                           |                           |                           | 1786          | 3              | -5.1               |
|                 | 1206 OKHALDHUNGA     | 27.31              | 86.50              | 1720      | 17.6               | 2              | -0.017                    | 0.042                     | 0.000                     | 1017          | 2              | -23.4 $^{\circ}$   |
|                 | 1210 KURULE GHAT     | 27.13              | 86.41              | 497       |                    |                |                           |                           |                           | 1324          | 4              | 15.9               |
|                 | 1211 KHOTANG BAZAR   | 27.03              | 86.83              | 1295      |                    |                |                           |                           |                           | 1402          | 6              | 10.4               |
|                 | 1222 DIKTEL          | 27.21              | 86.80              | 1623      |                    |                |                           |                           |                           | 4537          | 6              | -54.3 **           |
|                 | 1301 NUM             | 27.55              | 87.28              | 1497      |                    |                |                           |                           |                           | 1469          | 0              | -1.1               |
|                 | 1303 CHAINPUR (EAST) | 27.28              | 87.33              | 1329      | 19.1               | 0              | -0.127 *                  | 0.024                     | -0.064 $^{\circ}$         | 1540          | 4              | -3.7               |
|                 | 1304 PAKHRIBAS       | 27.05              | 87.28              | 1680      | 16.7               | 0              | -0.005                    | 0.036 *                   | 0.015                     | 942           | 6              | -9.2 $^{\circ}$    |
|                 | 1307 DHANKUTA        | 26.98              | 87.35              | 1210      | 20.0               | 0              | -0.002                    | 0.153 ***                 | 0.071 ***                 | 1052          | 6              | -13.1 $^{\circ}$   |
|                 | 1314 TERHATHUM       | 27.13              | 87.55              | 1633      | 18.2               | 10             | 0.033                     | 0.066 $^{\circ}$          | 0.049 **                  | 2531          | 5              | -41.9 *            |
|                 | 1317 CHEPUWA         | 27.46              | 87.25              | 2590      |                    |                |                           |                           |                           | 1429          | 6              | -22.9 $^{\circ}$   |
|                 | 1322 MACHUWAGHAT     | 26.96              | 87.16              | 158       |                    |                |                           |                           |                           | 2347          | 1              | 2.6                |
|                 | 1403 LUNGTHUNG       | 27.55              | 87.78              | 1780      |                    |                |                           |                           |                           | 1966          | 3              | -11.6              |
|                 | 1405 TAPLEJUNG       | 27.35              | 87.66              | 1732      | 16.6               | 1              | 0.060 *                   | 0.085 **                  | 0.071 **                  | 1287          | 2              | -13.6 *            |
| 1419 PHIDIM     | 27.15                | 87.75              | 1205               | 21.2      | 7                  | 0.047 *        | 0.082 **                  | 0.067 **                  |                           |               |                |                    |
| MEAN            | 27.33                | 87.00              | 1587               | 17.9      | 2                  | 0.003          | 0.060 $^{\circ}$          | 0.029 $^{\circ}$          | 1527                      | 4             | -11.1          |                    |
| PYRAMID         | 27.96                | 86.81              | 5035               | -2.4      | 0                  | 0.072 ***      | 0.009                     | 0.044 *                   | 449                       | 0             | -13.7 ***      |                    |
| KO-N<br>(TIBET) | DINGRI               | 28.63              | 87.08              | 4,302     | 3.5                | 0              | 0.037 $^{\circ}$          | 0.041 $^{\circ}$          | 0.037 *                   | 309           | 0              | -0.1               |
|                 | NYALAM               | 28.18              | 85.97              | 3,811     | 4.1                | 0              | 0.032 $^{\circ}$          | 0.036 $^{\circ}$          | 0.036 $^{\circ}$          | 616           | 0              | -0.2               |
|                 | MEAN                 | 28.41              | 86.53              | 4,057     | 3.8                | 0.1            | 0.034 $^{\circ}$          | 0.039 *                   | 0.037 *                   | 463           | 0              | -0.1               |

1443

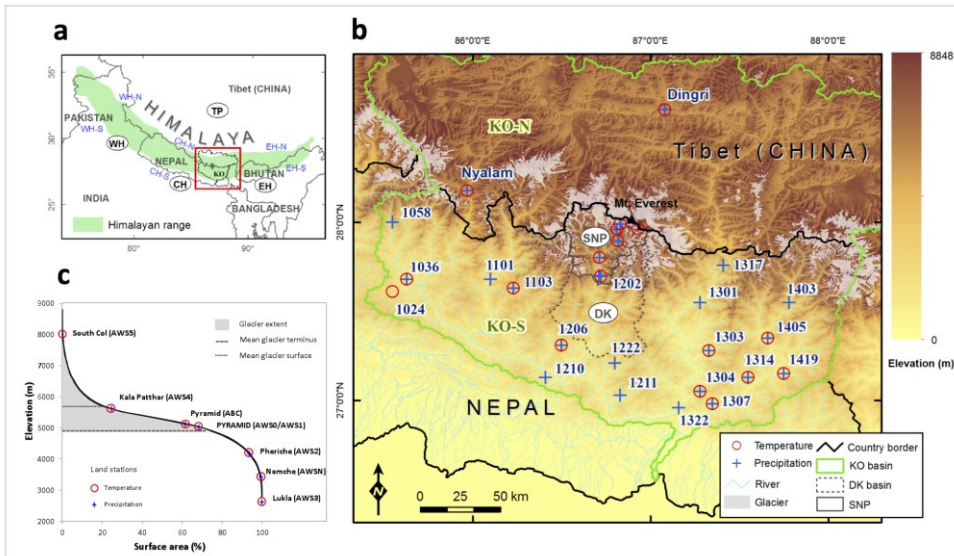
1444

1445 Table 3. Descriptive statistics of the Sen's slopes on a seasonal basis for minimum,  
 1446 maximum, and mean air temperatures and total precipitation of weather stations  
 1447 located in the Koshi Basin for the 1994-2012 period. The Nepali and Tibetan stations  
 1448 are aggregated as mean values. Level of significance ( $^{\circ}$   $p$ -value = 0.1, \*  $p$ -value = 0.05,  
 1449 \*\*  $p$ -value = 0.01, and \*\*\*  $p$ -value = 0.001). Annual and seasonal temperature trends  
 1450 are expressed as  $^{\circ}\text{C } \alpha^+ \underline{y}^{-1}$ . Annual precipitation trend is expressed as  $\text{mm } \alpha^+ \underline{y}^{-1}$ , while  
 1451 the seasonal precipitation trends are in  $\text{mm (4 months) } \alpha^+ \underline{y}^{-1}$ .

| Location                           | Minimum Temperature |                    |                      |                      | Maximum Temperature |         |                    |                    | Mean Temperature   |         |                     |                     | Total Precipitation |                    |                    |                      |
|------------------------------------|---------------------|--------------------|----------------------|----------------------|---------------------|---------|--------------------|--------------------|--------------------|---------|---------------------|---------------------|---------------------|--------------------|--------------------|----------------------|
|                                    | Pre-                | Monsoon            | Post-                | Annual               | Pre-                | Monsoon | Post-              | Annual             | Pre-               | Monsoon | Post-               | Annual              | Pre-                | Monsoon            | Post-              | Annual               |
| SOUTHER KOSHI BASIN (KO-S, NEPAL)  | 0.012               | -0.005             | -0.001               | 0.003                | 0.076 <sup>*</sup>  | 0.052   | 0.069 <sup>*</sup> | 0.060 <sup>*</sup> | 0.043              | 0.020   | 0.030               | 0.030 <sup>*</sup>  | 0.8                 | -8.6               | -2.5               | -11.1                |
| PYRAMID (NEPAL)                    | 0.067 <sup>*</sup>  | 0.041 <sup>*</sup> | 0.151 <sup>***</sup> | 0.072 <sup>***</sup> | 0.024               | -0.028  | 0.049              | 0.009              | 0.035              | 0.015   | 0.124 <sup>**</sup> | 0.044 <sup>**</sup> | -2.5 <sup>**</sup>  | -9.3 <sup>**</sup> | -1.4 <sup>**</sup> | -13.7 <sup>***</sup> |
| NORTHERN KOSHI BASIN (KO-N, TIBET) | 0.042 <sup>*</sup>  | 0.019              | 0.086 <sup>*</sup>   | 0.034 <sup>*</sup>   | 0.023               | 0.030   | 0.071 <sup>*</sup> | 0.039 <sup>*</sup> | 0.042 <sup>*</sup> | 0.013   | 0.084 <sup>*</sup>  | 0.037 <sup>*</sup>  | 2.2                 | 0.4                | -3.3 <sup>*</sup>  | -0.1                 |

1452

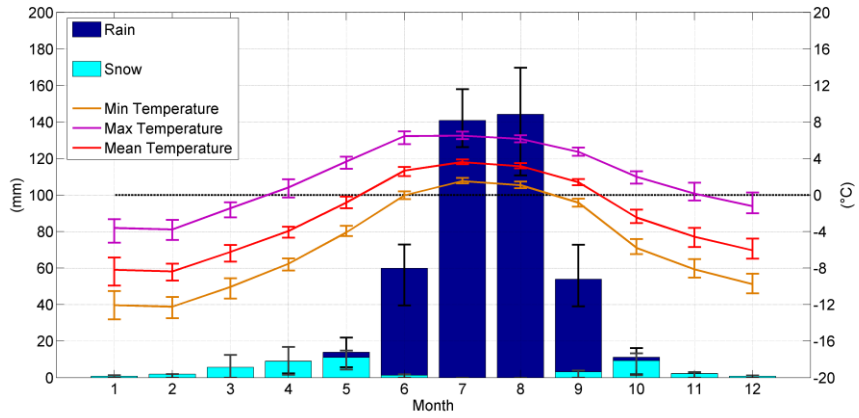
1453



1454

1455 *Figure 1. a) Location of the study area in the Himalaya, where the abbreviations WH,*  
 1456 *CH, EH represents the Western, Central and Eastern Himalaya, respectively (the*  
 1457 *suffixes -N and -S indicate the northern and southern slopes). b) Focused map on the*  
 1458 *spatial distribution of all meteorological stations used in this study, where KO and DK*  
 1459 *stand for the Koshi and Dudh Koshi Basins, respectively; SNP represents the*  
 1460 *Sagarmatha National Park. c) Hypsometric curve of SNP (upper DK Basin) and*  
 1461 *altitudinal glacier distribution. Along this curve, the locations of meteorological*  
 1462 *stations belonging to PYRAMID Observatory Laboratory are presented.*

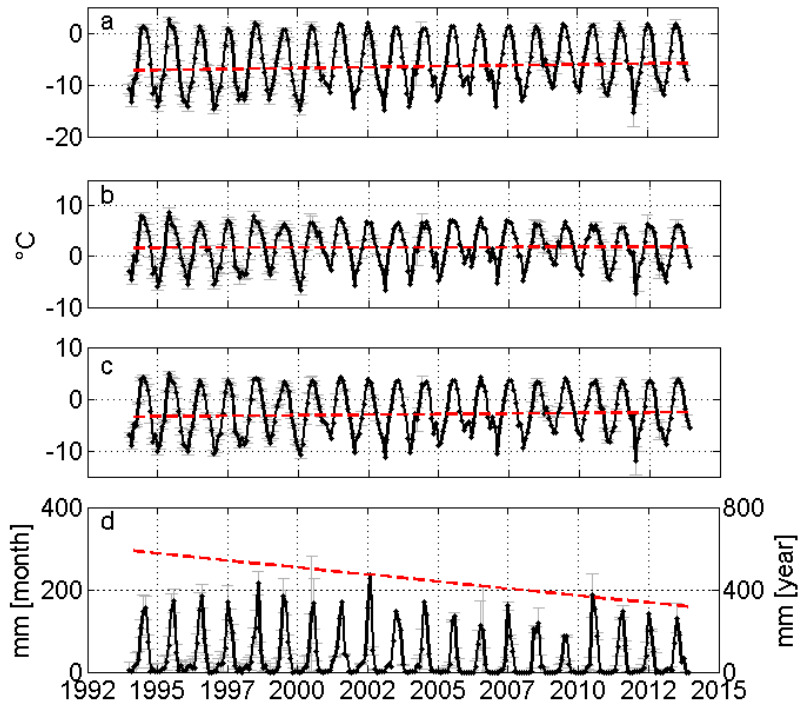
1463



1464

1465 *Figure 2. Mean monthly cumulated precipitation subdivided into snowfall and rainfall*  
 1466 *and minimum, maximum, and mean temperature at 5050 m a.s.l. (reference period*  
 1467 *1994-2013). The bars represent the standard deviation.*

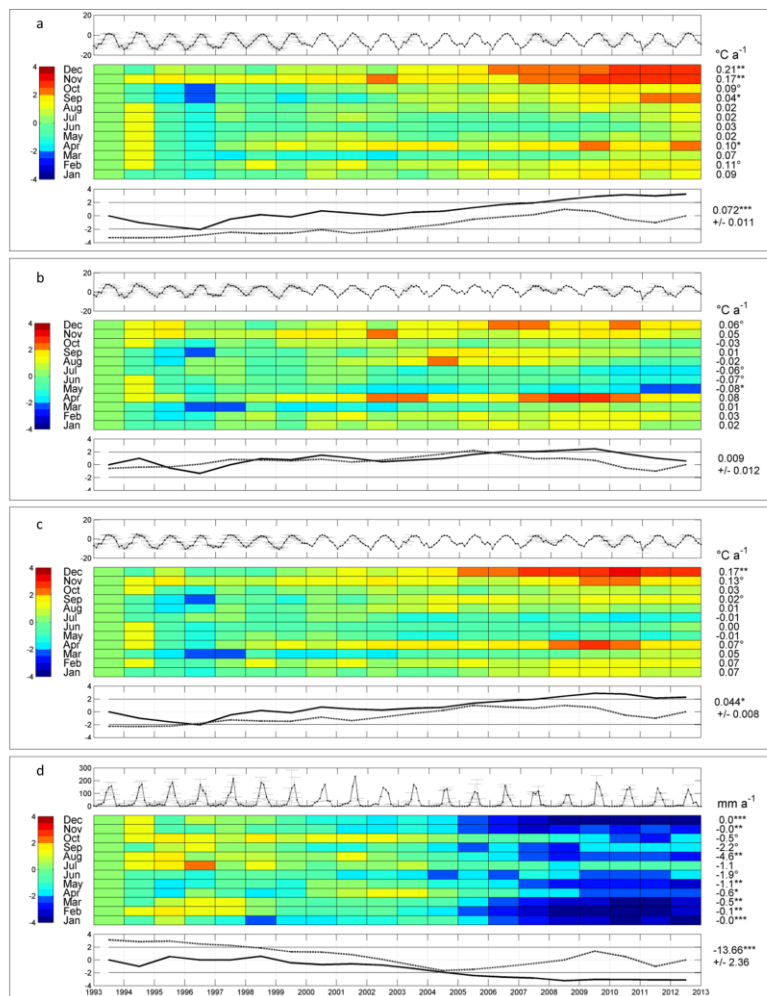
1468



1469

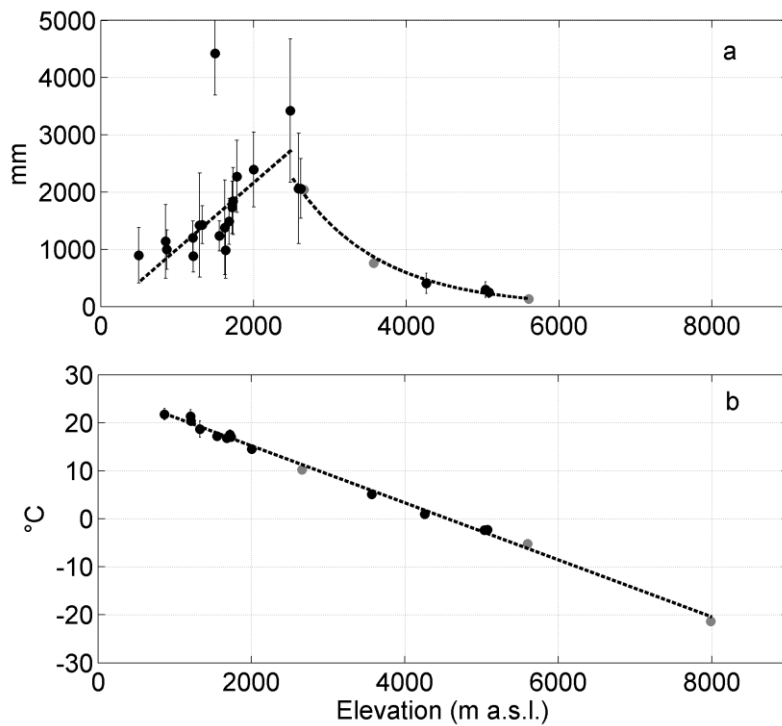
1470 *Figure 3. Temperature and precipitation monthly time series (1994-2013) reconstructed*  
 1471 *at high elevations of Mt. Everest (PYRAMID): minimum (a), maximum (b), and mean*  
 1472 *temperature (c), and precipitation (d). Uncertainty at 95% is presented as gray bar. The*  
 1473 *red lines represents the robust linear fitting of the time series characterized by the*  
 1474 *associated Sen's slope. According to Dytham (2011), the intercepts are calculated by*  
 1475 *taking the slopes back from every observation to the origin. The intercepts used in here*  
 1476 *represent the median values of the intercepts calculated for every point (Lavagnini et*  
 1477 *al., 2011). For precipitation the linear fitting refers at the right axis.*

1478



1479

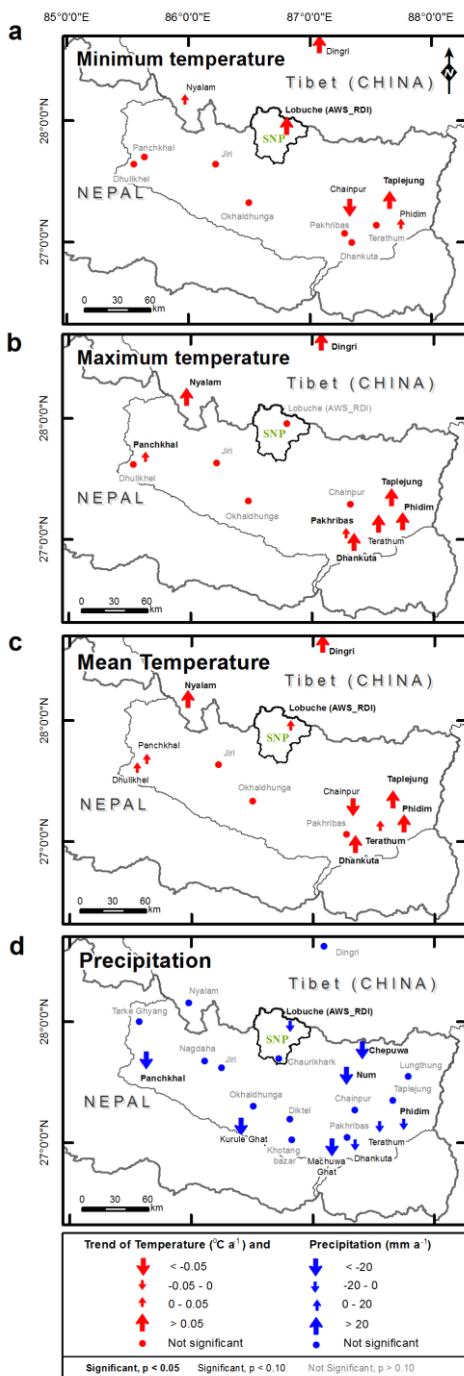
1480 *Figure 4. Trend analysis for a) minimum, b) maximum, and c) mean air temperatures*  
 1481 *and d) total precipitation in the upper DK Basin. The top graph of each meteorological*  
 1482 *variable shows the monthly trend (dark line) and uncertainty due to the reconstruction*  
 1483 *process (gray bars). The central grid displays the results of the sequential Mann-*  
 1484 *Kendall (seqMK) test applied at the monthly level. On the left, the color bar represents*  
 1485 *the normalized Kendall's tau coefficient  $\mu(\tau)$ . The color tones below  $-1.96$  and above*  
 1486  *$1.96$  are significant ( $\alpha = 5\%$ ). On the right, the monthly Sen's slopes and the relevant*  
 1487 *significance levels for the 1994-2013 period ( $^{\circ}$   $p$ -value = 0.1, \*  $p$ -value = 0.05, \*\*  $p$ -*  
 1488 *value = 0.01, and \*\*\*  $p$ -value = 0.001). The bottom graph plots the progressive (black*  
 1489 *line) and retrograde (dotted line)  $\mu(\tau)$  applied on the annual scale. On the right, the*  
 1490 *annual Sen's slope is shown for the 1994-2013 period. [MATLAB® script is available at](http://www.irsas.cnr.it/Docs/Code/MSeqMK.m)*  
 1491 *<http://www.irsas.cnr.it/Docs/Code/MSeqMK.m>*



1492

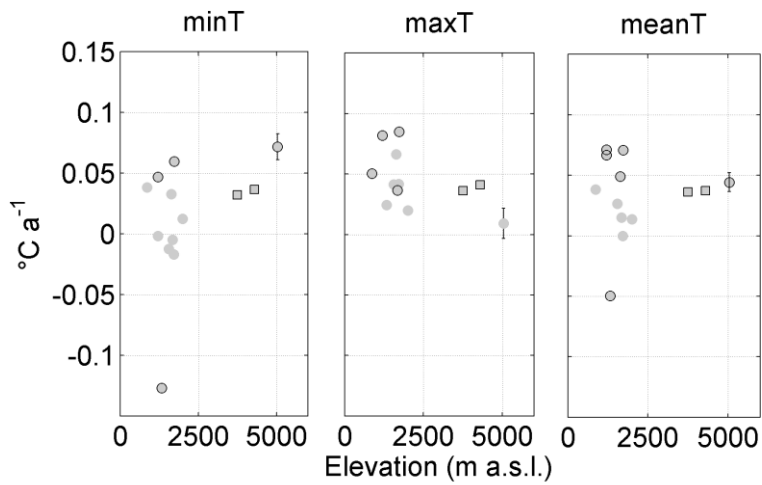
1493 | *Figure 5. Lapse rates of (a) total annual precipitation in the Koshi Basin for the last 10*  
 1494 *years (2003-2012) mean annual air temperature and (b) mean annual air temperature*  
 1495 *total annual precipitation in the Koshi Basin for the last 10 years (2003-2012). The*  
 1496 *daily missing data threshold is set to 10%. Only stations presenting at least 5 years of*  
 1497 *data (black points) are considered to create the regressions (the bars represent two*  
 1498 *standard deviations). Gray points indicate the stations presenting less than 5 years of*  
 1499 *data.*

1500



1501

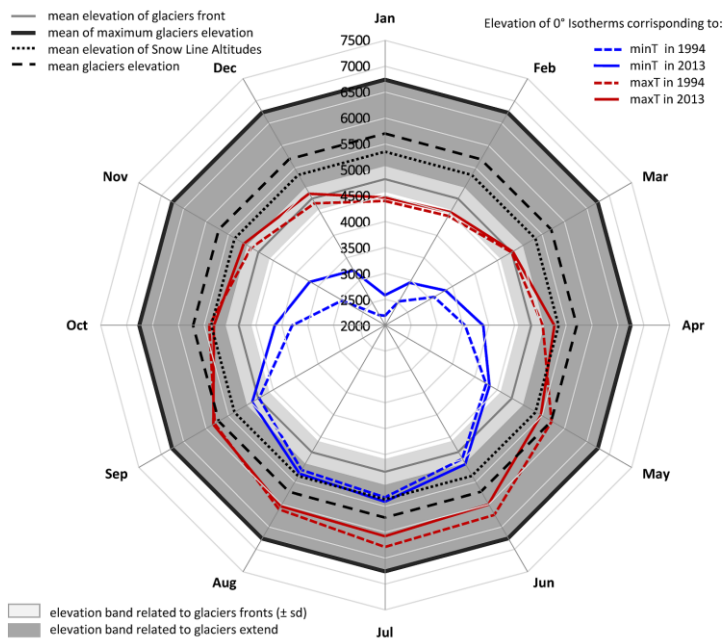
1502 *Figure 6. Spatial distribution of the Sen's slopes in the Koshi Basin for minimum (a),*  
 1503 *maximum (b), and mean (c) air temperature and (d) total precipitation for the 1994-*  
 1504 *2013 period. Data are reported in Table 2.*



1505

1506 *Figure 7. Elevation dependency of minimum (a), maximum (b), and mean (c) air*  
 1507 *temperatures with the Sen's slopes for the 1994-2013 period. The circle indicates*  
 1508 *stations with less than 10% of missing daily data, and the star indicates stations*  
 1509 *showing a trend with p-value < 0.1. The red marker represents the trend and the*  
 1510 *associated uncertainty (two standard deviations) referred to the reconstructed time*  
 1511 *series for the AWSI station (Pyramid). Data are reported in Table 2.*

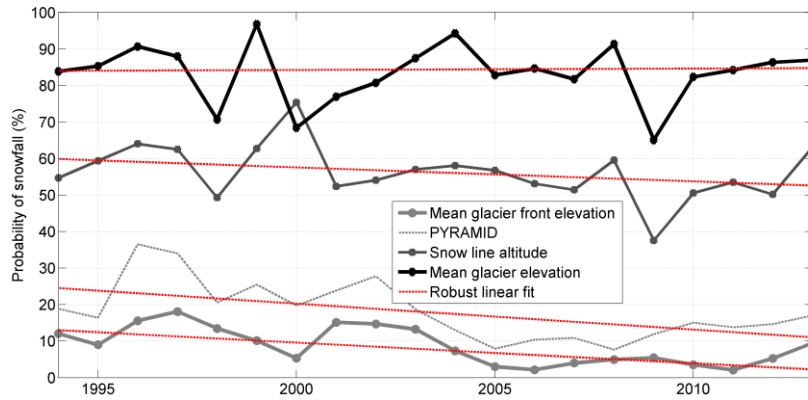
1512



1513

1514 *Figure 8. Linkage between the temperature increases and altitudinal glacier*  
 1515 *distribution. The 0 °C isotherms corresponding to the mean monthly minimum and*  
 1516 *maximum temperature are plotted for the 1994 and 2013 years according the observed*  
 1517 *T trends and lapse rates.*

1518



1519

1520 *Figure 9. Trend analysis of annual probability of snowfall on total cumulated*  
 1521 *precipitation. The red lines represents the robust linear fitting of the time series*  
 1522 *characterized by the associated Sen's slope (more details in the caption of Fig. 3).*